STATE RESEARCH CENTER OF RUSSIA

INSTITUTE FOR HIGH ENERGY PHYSICS

REPORT

Pre–engineering Design for the Technical Components of the NuMI Beams

(Task D of the Accord between FNAL and IHEP)

A.Abramov, S.Denisov, P.Galkin, N.Galyaev, V.Garkusha,
A.Kharlamov, Yu.Khodyrev, S.Knyazev, E.Lomakin,
F.Novoskoltsev, A.Ryabov, V.Seleznev, Z.Sharifullin,
E.Ustinov, V.Zapolsky, V.Zarucheisky

Protvino 1997

Contents

1 Technical Characteristics of Target Station Elements **3**
1.1 Target Head 3
1.1.1 Design Parameters 3
1.1.2 Thermo–mechanical Analysis 6
1.2 Target Unit 7
1.3 Alignment Plant 11
1.3.1 Design characteristic 11
1.3.2 Technical Parameters 12
1.4 Detector Design Parameters 15

2 NuMI Beam Focusing Systems with Conical and Parabolic Horns (preliminary results) **40**

3 Parabolic Lenses **44**
3.1 General layout 44
3.2 Initial Installation of FD and Replacement of failed FD assembly 45
3.3 FD assembly 46
3.3.1 Inner conductor 47
3.3.2 Outer conductor 47
3.3.3 Water cooling 48

1 Technical Characteristics of Target Station Elements

More detailed characteristics (geometry, sizes, selected materials, assembly and operating conditions) for designs of the basic equipment of the target station are given in this Report. The choice of described designs was the result of the compromise between inconsistent requirements together with some simplifying assumptions and absence of enough data about materials and technology. Therefore, some of the presented technical solutions may change when either conditions of this compromise is changed or more detailed engineering design is performed.

In some cases the final choice of designs (first of all for the target unit) can be made only after manufacturing the prototypes and carrying out of preliminary tests in a beam.

1.1 Target Head

1.1.1 Design Parameters

Figure 1.1 shows the configuration and sizes of target head (cross section) for the WBB target unit in the framework of the fin–target design philosophy. This philosophy based on use of conductive cooling, as the main method of cooling of these targets.

There are two most important features of this target head:

- The target head itself and its support (unlike variants which were presented in the previous IHEP Reports [1] and [2]) are combined together as one component. It permits to increase the efficiency of cooling and to simplify its fixture.
- High–strength beryllium alloy (for example, modified, forged I–400 alloy of Brush Beryllium Co., Cleveland) is used as a target material. The strength on destruction and plasticity of this alloy is 2–3 times larger then respective values for ordinary technical beryllium.

Figure 1.1 also explains methods of an alignment and a fixture of the target head (1) on the base plate (8) of the target unit. Table 1.1 lists the target head elements and their main parameters. The target head has an electrically insulating layer between its bottom and a base plate. Besides,

there is the insulation layer between pressing bolts (2) and a lower part of the target head. A Kapton H film or an aluminium anodized foil is foreseen as electrical insulation. In a contact surface between beryllium and aluminium an additional steel foil may be placed to compensate the influence of the difference of thermal expansion coefficients of these materials.

Position	Name	Material	Number	Note
1	Target Head	Beryllium alloy I–400 [2], modified	5	
2	Bolt to press	Titanium or Steel	50	
3	Bolt to fix	Titanium or Steel	30	
4	Insulating Film	KAPTON H [2]	10	B 8 mm
5	Bracket	Titanium alloy VT6 [1]	10	
6	Insulating Film	KAPTON H [2]	5	B 40 mm
7	Screw to align	Steel	20	
8	Base Plate	Aluminium alloy	1	

Table 1.1: List of target head elements. [1] – Russian, [2] – American marks.

Screws (7) are used for an alignment of target segments (four screws on each target segment) in a horizontal plane when target unit is assembled. Requirements to vertical alignment are reduced and so it is provided with the help of gaskets.

Optimization of secondary particles yields, thermal loads, cooling methods and thermo-mechanical stresses which were obtained in the process of their study and calculations permitted to choose the geometry of the target head, shown in Figure 1.1. Such geometry is the most optimal for initial (upstream) segments of the target. The total length along z-axis for their arrangement does not exceed 0.5 m. Initial segments have the largest thermal loads and thermo-mechanical stresses, while the beam radius of necessary (accepted by focusing system) secondary particles does not exceed 20 mm. For next segments the size marked as * in Figure 1.1 may be decreased or transverse slits in this part of the segment should be made in order to reduce the secondary particles absorption, because the beam radius of necessary secondary particles is increased at the downstream target end up to 70 mm. Such modifications of a configuration of these segments are

possible because for them the energy deposition is considerably less than for initial segments (see below, Table 1.4). In comparison with the cylindrical target the chosen fin–target configuration has the following advantages:

- Layout, assembly and maintenance of the target unit get considerably simpler, in particular, there is no need in helium cooling. In addition to conductive cooling an air cooling can be used.
- There are vast opportunities to modify a configuration and a location of separate segments in the longitudinal direction in order to increase efficiency of cooling and decrease thermo–stresses.
- It permits to vary the size of a spot of the proton beam on the target without changes of efficiency of its interaction with the target.
- Losses in a secondary particles yield due to partial failure of the target head, can be minimized by moving of the target upwards.

It is assumed for described target to use the proton beam with the elliptical form of a spot. The R.M.S. value for horizontal size of the beam σ_x is equal to 0.8 mm and is constant. The vertical R.M.S. value σ_y may be varied between 1.6 and 2.0 mm. The choice of the final value σ_y is depending on properties of the definite mark of beryllium alloy and technology of manufacturing of the target head (in particular, a damage limit connected with metal fatigue changes by the factor of two depending on the state of its surface).

Melting temperature	1284 °C
Density	1.845 g/cm^3
Specific Heat c_p	1.78 J/g/°C
Coeff. of thermal expansion α_p	$10.8 \cdot 10^{-6}$/°C
Thermal Conductivity λ	1.8 W/cm/°C
Modulus of elasticity E	300 GPa
Tensile strength σ_b	838 MPa *)
Yield strength σ_{02}	704 MPa *)
Relative lengthening δ	5.95%
Poisson's ratio ν	0.025

Table 1.2: Properties of Beryllium at 20°C.
*) – beryllium alloy I–400, modified and forged.

Table 1.2 lists the thermophysical and mechanical properties of beryllium used for these calculations. A dependence of the beryllium properties on temperature was taken into account (see Figures 1.2 and 1.3).

1.1.2 Thermo–mechanical Analysis

For the chosen target the detailed analysis of transient thermal problem and mechanical phenomena were performed. The energy deposited by the proton beam in the target material has been calculated using the Monte Carlo MARS program [3]. In Figure 1.4 the three–dimensional diagram illustrates the character of the distribution of the energy deposition density in cross section (on x, y axes; $x = y = 0$ corresponds to beam position) of the first segment for the region of the maximum energy density in a longitudinal direction ($z_{max} \simeq 6$ cm). The segment is compact (hard case). In this Figure the energy density is expressed in relative units. The maximum value of the energy density (per one proton) is equal to 0.091 GeV/cm^3 if σ_y=1.6 mm and 0.072 GeV/cm^3 if σ_y=2.0 mm (σ_x=0.8 mm). As to energy density which is average on segment length (19.3 cm), its value is equal (on a z-axis) to 0.082 GeV/cm^3 and 0.063 GeV/cm^3, respectively.

For temperatures calculations the non–stationary and nonlinear thermal task was solved, using the two–dimensional finite–element program HEAT2D of the HAST package [4]. It became possible because heat generation rate does not depend on longitudinal z-coordinate. Besides, the considered problem has a symmetry plane $x = 0$, that's why the finite-element model was designed only for half-section of the target. It's assumed that the proton beam has Gaussian x- and y-profiles, an intensity of $4{\cdot}10^{13}$ ppp, total spill time of 1.4 ms and cycle time of 1.9 s. Spill depends on a time like $\sim t^2(t-1.4{\cdot}10^{-3})^2$ function with normalization to 1 for $0 \leq t \leq 1.4{\cdot}10^{-3}$s. It's was also assumed that temperature of surrounding gas and cooling water is equal to 28°C. The value of transverse heat coefficient is $\alpha_w = 10000$ W/m^2/°C. Beside of conductive cooling, forced convection with convection coefficient $\alpha_g = 50$ W/m^2/°C and radiation cooling were taken into account. For simulation of radiation losses the Stefan–Boltzman law was used where emissivity ε is equal to 1 (the black body approach).

The results of these temperature calculations are shown in Figure 1.5. At steady state with additional forced convection and radiation cooling the maximum temperatures are equal to 171°C at the spill beginning and

281°C just after the spill end, so a temperature rise is 110°C. If the additional cooling is absent, corresponding values are equal to 201, 308 and 107°C. The evolution of the maximum temperature of the target in time for both methods of cooling is shown in Figure 1.6. The steady state is reached within $75 \div 100$ cycles. The temperature gradient is defined only by the height and width of the target and by thermal conductivity of target material (by thermal resistivity of the target).

To take into account the fin target length in calculation of quasi-static thermal stress, the three–dimensional finite elements code STRESS3D of the HAST package [4] was used. Due to the symmetry only one quarter of full model was considered. Calculations of stress for targets of different lengths, L = 4, 8, 12, 20, 40 and 60 mm, were performed.

The temperature distribution obtained from two–dimensional transient thermal analysis was transferred to the node coordinates of a three–dimensional finite-element mesh. We assumed that the bottom target surface is constraint-free in $x-z$ plane but fixed in y-direction. The dependence of the thermal expansion coefficient on temperature was taken into account. Calculations of stress were performed for instant of time with maximum temperature state (at the beam spill end).

The results are given in Figures 1.7–1.10 for steady state. They show distributions of stress components σ_{xx}, σ_{yy}, σ_{zz} and equivalent stress σ_{eq} (von Mises) at the middle cross-section of the target having the length of 12 mm. Note that values of shearing stress components are negligible and were not given here. Equivalent stress σ_{eq} and longitudinal stress component σ_{zz} at the most critical target point ($x = y = 0$, $z = z_{max}$) as functions of the target length are shown in Figure 1.11. The value of σ_{zz} increases when the length of a target is increased, so an upper limit of the target length exists. Safety factor of the fatigue damage limit may be reached if modified beryllium alloy I–400 is used. As to temperature deformations caused by passing of the axial proton beam, the most considerable of them is the deformation in a direction of an y-axis (upwards), which reaches the value of 0.065 mm.

1.2 Target Unit

The target head described in the previous section allows to realize the variant of the target unit which is rather simple and light. It was conditioned

by a chosen type of the target and a refuse from the helium cooling. The design of the target unit at that approach is shown in Figures 1.12–1.14. The basic elements of the target unit and their main parameters are given in Table 1.3.

Position	Name	Material	No.	Note
1	Box	Aluminium alloy AMG–4 [1)])	1	
2	Box Casing	Aluminium alloy AMG–4 [1)]	1	
3	Fin Target	Beryllium alloy I–400 [2)], modified	5	
4	Bracket	Titanium alloy VT6 [1)]	10	
5	Insulating Film	KAPTON H [2)]	5	B 40 mm
6	Insulating Film	KAPTON H [2)]	10	B 8 mm
7	Window	Titanium alloy VT6 [1)]	1	ø140 mm d40 μm
8	Window	Titanium alloy VT6 [1)]	1	ø70 mm d40 μm
9	Air Collector	Aluminium alloy AMG–4 [1)]	2	ø30 mm
10	Flange	Aluminium alloy AMG–4 [1)]	2	ø90 mm, ø160 mm

Table 1.3: List of target unit elements. [1)] – Russian, [2)] – American marks.

The longitudinal structure of the target has five identical segments, because this structure for the target was accepted here. The length of each segment is equal to 193 mm. Gaps between segments are identical too and each of them is equal to 185 mm. The total length of the target material is equal to 965 mm; it approximately corresponds to 2.2 nuclear interaction length of protons. The geometrical length of a target is equal to 1715 mm.

As one could see, the design of the target that was shown here, allowed to use segments homogeneous on length and segments consisted of several parts. Table 1.4 summarizes calculation results of energy deposition in the described target, which allow to compare thermal loads in all its 5 segments. Energy deposition are given for total intensity of one proton beam spill.

Number of a segment	1	2	3	4	5
Energy deposition density on an axis of the beam averaged by the length of the segment q_0, kJ/cm^3	0.41	0.29	0.19	0.12	0.07
Total energy deposited in the top part of the segment $Q_{s.top}$, kJ (dY = 24 mm from the top)	1.11	0.95	0.71	0.50	0.35
Total energy deposited in the segment Q_{seg}, kJ	1.15	1.05	0.84	0.64	0.53
Total energy deposited in the target Q_{tar}, kJ	4.21				

Table 1.4: Energy deposited by the proton beam with intensity $4{\cdot}10^{13}$ ppp for each target segment.

Target parameters			Proton beam size	π^+ yield, rel.unit (θ=40 mrad)		WBB Far detec. ν_μ event rate, rel.unit
Material and configuration	Sizes, cm $L_T\times\phi$ $L_T\times W\times H$	Segments No.$\times L_S$, cm and ρ, g/cm^3	$\sigma_x\times\sigma_y$, cm^2	E_π, GeV 15–45	E_π, GeV 35–45	
C–cylinder *)	170×0.38	1×170 1.2	0.07×0.07	1	1	1
C–cylinder [5]	156×0.40	8×12.5 1.81	0.09×0.09	0.926	0.92	0.99
Be–cylinder *)	190×0.54	1×190 0.95	0.12×0.12	0.963	0.95	
Be–cylinder	171×0.54	5×19.3 1.85	0.12×0.12	0.939	0.92	0.95
Be–fin *)	190×0.41×5.4	1×190 0.95	0.08×0.16	0.987	0.96	0.93
Be–fin	171×0.41×7.4	5×19.3 1.85	0.08×0.16	0.968	0.93	0.94
Be–fin	183×0.41×7.4	10×9.7 1.85	0.08×0.16	0.981	0.95	
Be–fin *)	190×0.41×5.4	1×190 0.95	0.08×0.20	0.983	0.95	0.92
Be–fin	171×0.41×7.4	5×19.3 1.85	0.08×0.20	0.965	0.93	0.90
Be–fin	183×0.41×7.4	10×9.7 1.85	0.08×0.20	0.971	0.94	

Table 1.5: Comparison between the calculated production efficiency for different targets (*) – hypothetical case).

A production efficiency of this target compared with another considered target are given in Table 1.5. A production efficiency was determined on positive pion yields as well as neutrino event rate at the far detector. The pion yields were calculated by a method described in previous IHEP Report [2]. The total number of neutrino events/(kTon*Yr) at the far detector for the 3L1/2L3 focusing system described in IHEP Report [1] were calculated using the Fermilab beam simulation package GNuMI.

Computation results given in Table 1.5 show that production efficiency is scarcely affected by longitudinal configuration of the target. Therefore the choice of longitudinal structure of the target is defined by stresses and target manufacturing.

Box base (Figures 1.13 and 1.14, pos.1) is a plate with overall sizes $200\times20\times2000$ mm^3 (width$\times$thickness$\times$length). In the bottom plane of the plate ribs with sizes $8\times20\times2000$ mm^3 (width$\times$height$\times$length) are placed. The base is made from the deformable aluminium alloy AMG–4, which was not strengthened by thermal working. This alloy has strength limit of 300 MPa and flow stress limit of 150 MPa. The protective casing is made from the same aluminium alloy and it has a hemisphere form in a cross section. There are two titanium windows (alloy VT6) with thickness of 40 μm and diameters of 70 and 140 mm, respectively at the front and back casing ends.

The protective casing hermetically connects to the base. The thickness of the lateral casing wall is equal to 1 mm. The average thermal power emitted from the base and casing caused by the irradiation of the secondary particles beam, is equal to 1 kW and 90 W, respectively. Water is used for cooling and thermostabilisation of the box base and for conductive cooling of the target. There are three channel in the box base body for circulation of cooling water. Water is supplied to the central channel with cross section 40×5 mm^2, and leaded out to lateral channels with cross section 20×5 mm^2 in each channel.

These channels connected to external pipe–line through connecting pipes, which got off through the bottom surface of the base in its front part. For water flow rate of 3 m/s at the bounder with the target, the heat emission factor of 10000 W/m^2/°C is provided. Water consumption is equal to 0.6 l/s (is about 2 m^3/h). The average water heating in this case does not exceed 1°C, while maximum temperature gradients in the material of the box base don't exceed 1°C/cm. The cooling of the casing is provided

with an external air flow, which cools elements of the "hot zone".

Dry and pure air circulating in the closed autonomous system is used for cooling of the target. This air supplies to collectors placed inside the box in both sides of the target. Air streams which flow with rate 4 m/s in a direction of the target are arose with help of jets. The total jet section is equal to 40 cm^2. The air consumption in this case is of the order ~ 60 m^3/h at normal conditions.

1.3 Alignment Plant

1.3.1 Design characteristic

Side, top and front views of the alignment plant are shown in Figures 1.15–1.17. This plant is used for movement, digitizing of the values of movement and accurate positioning of the target unit (TU) placed in the "hot zone". The plant allows to carry out a calibration both in an automatic and semi-automatic operation mode and replacement of the TU. The plant has following parameters:

TU movement range:	
in axes y and z	50 mm
in angles φ_y and φ_z	5 mrad
Resolution:	
measuring system (2-channel system with absolute digital transducers of angular movements)	20 μm
calibration system (absolute analog induction transducers of linear movements)	30 μm
Accuracy of positioning by all coordinates	50 μm
Reproducibility of the position of the TU in a space	± 50 μm
Speed of movement	$1 \div 5$ mm/s
Servo-drives on all axes	DC electromechanisms without dead zone
Power consumption at 220 V, 50-60 Hz	1000 V·A
Weight	~ 500 kg

The principal elements list of the alignment plant are given in Table 1.6. Some technical parameters are given below.

N^0 p/p	Name	Material	Sizes, mm	Number
1	Alignment table	Rectangular steel pipe	2500×600×200	1
2	Primary frame	Rectangular steel pipe	2700×600×200	1
3	Rod	Cylindrical steel pipe	ø180, L=350	2
4	Target box			1
5	Servomechanism with DC motor			4
6	Transducer of channel precise position			4
7	Linear transducer of channel rough position			4
8	Guideway cylinder	Cylindrical steel pipe	ø200, L=150	2
9	Regulation jack			3
10	Support	Rectangular steel pipe		2
11	Suspension shaft	Steel	ø80/ø170, L=250	2
12	Suspension shaft	Steel X18H10T *)		3
13	Transducer of target box position			2
14	Support for transducer and beam monitor	Rectangular steel pipe		3
15	Guideway	Steel 40X, XBΓ *)	150×150×20	6
16	Flexible pipe	Steel X18H10T *)		4
17	Bracket	Steel 20 *)		2
18	X-carriage		200×150×150	1
19	Ball	Steel, ШX15 *)	ø60	3
20	Beam monitor box			1

Table 1.6: The principal elements of the alignment plant. *) – Russian mark.

1.3.2 Technical Parameters

Alignment table (pos.1). The alignment table is built from a rectangular steel pipe. The following components are placed on it:

- three polished plane guideways (pos.15, upper parts);
- unit for fastening of the carriage axle (pos.18) and a ball–screw (pos.19) of servomechanisms (pos.5) used for the alignment table movement in a horizontal plane;
- two polished base planes for fastening of servomotors of vertical movement with position transducers (pos.6,7).

Primary frame (pos.2). It's built as a welded alignment table from a rectangular steel pipe. The following components are placed on it:

- Three polished plane guideways (pos.15, lower parts) fixed in the top part of the frame.
- Carriage (pos.18) for horizontal movement of the alignment table.
- Base planes for alignment of calibration transducers of TU.

The suspension shafts (pos.11). Shafts are made as stepwise constructions. The upper parts of the shafts have demountable joints with rods (pos.3). The TU (pos.4) is fastened to its bottom parts with help of brackets (pos.17) to the underbody of the shafts. Top parts of shafts are connected to rods of vertical movement with help of bolt joint. There are some channels in the area of shafts for pipelines and electrowires. Shaft design parameters are:

Maximum diameter	170 mm
Minimum diameter	80 mm
Length	2000 mm
Weight	$\sim$ 50 kg

Jacks (pos.9). Screw jacks are used for manual alignment of the primary frame according to geodetic datum points. The jack design parameters are:

Screw movement	$\leq$ 100 mm
Maximum axial load	up to 1000 kg
Weight	10 kg

Servomotors (pos.5). Servodrivers with DC motors are used for linear and angular movement, accurate positioning of the TU. Two of them are used for horizontal and two others — for vertical movement of the TU. Design parameters are:

Maximum limit of ball–screw movement	120 mm
Step of the ballscrew pair	7.2 mm
Axial loading on the ballscrew:	
nominal/maximum	750/1250 kg
Ballscrew speed range	$1 \div 5$ mm/s
Maximum supply voltage	27 V
Current consumption	≤ 7 A
Overall sizes: diameter	110 mm
length	260 mm
Weight	≤ 5 kg

Measuring system. The position of the TU is measured by two channel measuring system (rough and accurate channels). Each servodrive is equipped with measuring system. The rough channel consists of a reducer and precise multiturn potentiometer. Precise potentiometer specifications are:

Number of turns (operating zone)	20
Rotation speed	up to 200 rev/min
Linearity of the output voltage	
at the operating range	$\pm 0.3\%$
Friction momentum at 20°C	2 g·mm
Potentiometer life	10000 cycles
Power consumption by the potentiometer	1 W
Overall sizes: diameter	20 mm
length	80 mm
Weight	50 g

The accurate channel consists of without dead zone reducer and photooptical absolute transducer. Design parameters are:

Maximum speed	6000 rev/min
Resolution	12 bits
Supply voltage	5, 10 V
Protection class	IP64
Overall sizes: diameter	80 mm
length	120 mm
Weight	0.8 kg

Measuring system of calibration. Periodic calibration of the TU, placed in a "hot zone" is provided with induction transducers in absolute coordinates.

This transducer was constructed at IHEP. It is possible to use it in radiation area. Parameters of the transducer are:

Voltage supply	36 V
Voltage frequency	400 Hz
Output slope	0.7 mV/μm
Load resistance	5 kOhm
Range of linearity	$\pm$80 mm
Overall sizes: diameter	70 mm
length	22 mm
Weight	0.5 kg

1.4 Detector Design Parameters

Task of beam diagnostics and tools for their realization were considered in the IHEP Report [2]. Designs and parameters of beam detectors, which are placed directly in the target enclosure are described here.

Secondary Emission Profilometers (SEPup-1, SEPup-2). They are used for measurements of the transversal profile of proton beams. The main feature of the proposed type of profilometers is that they work without electrical offset in gas environment. A profilometer design is shown in Figure 1.18. Element notifications in this Figure are: 1 and 3 – signal electrodes (W wire, ø40 μm) for horizontal and vertical planes, respectively; 2 – a shielding electrode (Ti – foil, 50 μm); 4 – insulating washer (Macor, American mark). Basic parameters are:

Operating range of beam intensity	$10^{11} \div 4{\cdot}10^{13}$ ppp
Number of planes of measurement	2
Number of channels in each plane	32
Step of winding	0.5 mm
Aperture	50×50 mm^2
Overall sizes	70×70×15 mm^3

SEPup-1 is placed in 8.7m before SEPup-2 for WBB and 1.5m for NBB. SEPup-2 is placed just before the target.

Charge Target Monitor (Q_{tar}–Budal monitor). It measures an efficiency of interaction of the proton beam with a target using charges from 5 electrically insulated segments. A layout of the insulated target with charge

gathering is shown in Figure 1.19. Element notifications in this Figure are: 1 – the insulating polyamide film; 2 – the twisted pair of wires MS 16–12–0.05 (Russian mark) with polyamide insulation. The basic properties of polyamide films are:

Thickness	40±4 μm
Density	1.42 g/cm^3
Module of elasticity	3 GPa
Tensile strength	80 MPa
Specific heat	1.1 J/g/°C
Thermal conductivity	$1.56 \cdot 10^{-3}$ W/cm/°C
Operating time at different temperatures	12 h at 400°C 3 months at 300°C unlimited time at 250°C
Electrical strength	200 MV/m
Radiation resistance	40000 Mrad

Du Pont produces in the USA an American analogue of the polyamide film. Its commercial mark called Kapton H.

Large–aperture Secondary Emission Profilometer (SEPdown). This detector measures the beam profile after the target. The profilometer design is given in Figure 1.20. Element notifications in this Figure are: 1 – vacuum-tight frame (stainless steel); 2 – vacuum 45-pin electrical feedthrough of the 2RMGD type (Russian mark); 3 – branch pipe for connection to vacuum pumps; 4 – up- and downstream windows (stainless steel foil, 100 μm); 5 – wire signal electrode (W–wire, ø40 μm). Basic parameters are:

Operating band of intensities	$10^{11} \div 10^{14}$ ppp
Number of measuring planes	2
Number of channels in each plane	32
Step of winding (including possible switching)	1 (2,4) mm
Aperture	ø200 mm
Overall sizes	250×250×50 mm^3
Operating vacuum	10^{-3} torr

Split-Plate Ion Chamber (SPIC). It is used for measurement of a symmetry of the distribution of secondary particles generated in the target and focused

by the optic system. The design of this device is shown in the Figure 1.21. Element notifications in this Figure are: 1 – frame (plastic); 2 – electrode system (Al, 1 mm); 3 – electrical plugs. Basic parameters are:

Operating volume of 4 sections	6.5 dm^3
Sensitivity	1.9 mkA·s/rad
Time resolution	300 μs
Band of linearity (5%)	10^5
Internal radius	100 mm
External radius	220 mm
Length on the beam-axis	150 mm

Secondary Emission Monitor (SEM). It is used for measurement (after absolute calibration by the current transformer) of intensity of the beam after the target. Multiplicity of the particle generation as well as the beam position and its halo are estimated using this device. The monitor design is shown in the Figure 1.22. Element notifications in this Figure are: 1 – vacuum-tight frame (stainless steel); 2 – input membrane (stainless steel foil, 100 μm); 3 – electrode system (stainless steel, 20 μm); 4 – vacuum 20-pin electrical connector (metalceramic, non-standard manufacturing); 5 – branch pipe for connection to vacuum pumps. Basic parameters are:

Operating range of beam intensity	$10^{11} \div 10^{14}$ ppp
Accuracy of measurement	$\pm 2\%$
Aperture	ø150 mm
Length along the beam-axis	150 mm
Vacuum	10^{-6} torr
Number of signal electrodes	7
Amount of matter in a beam	65 mg/cm^2

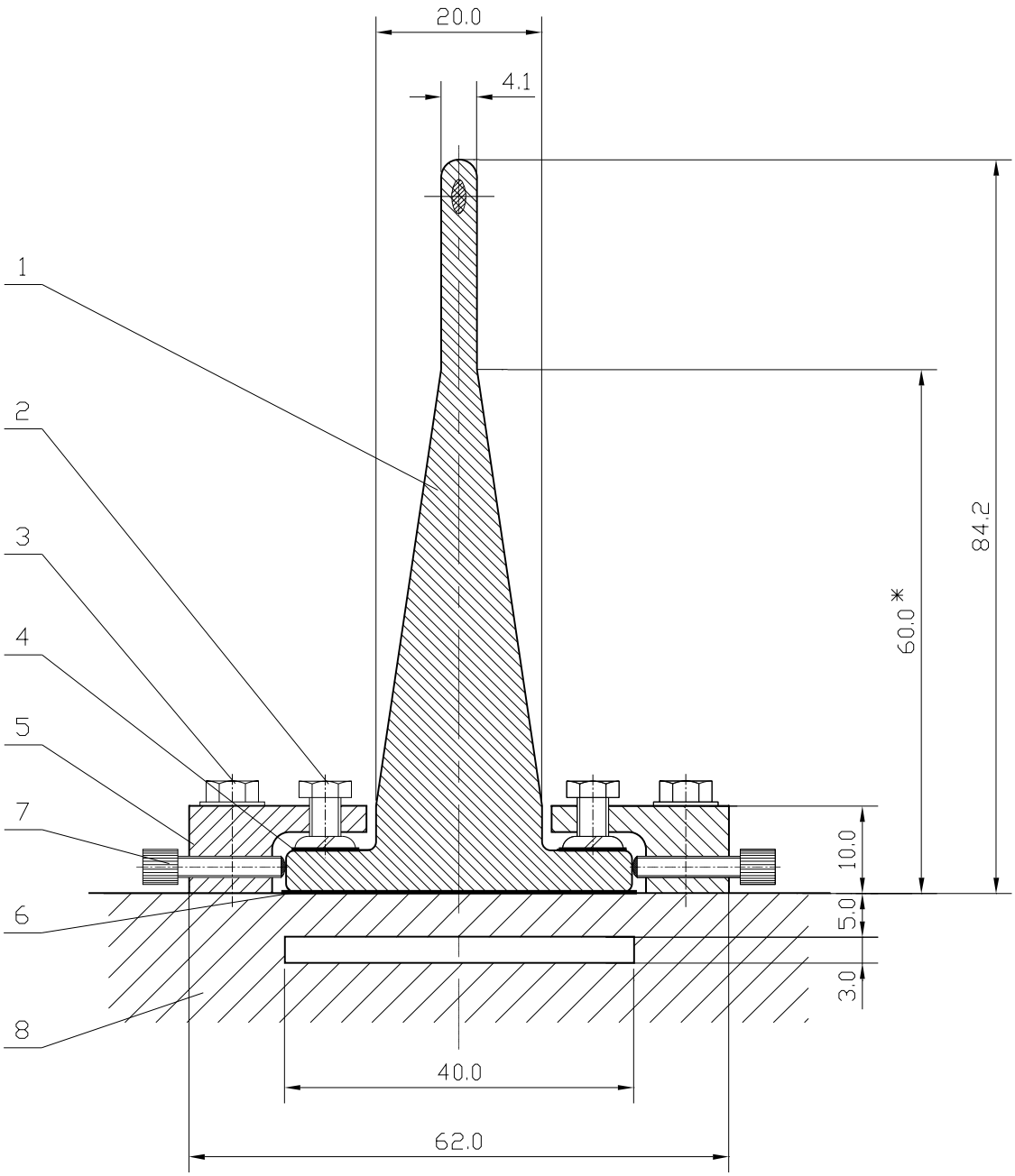

Figure 1.1: Cross-section view of the first target segment.

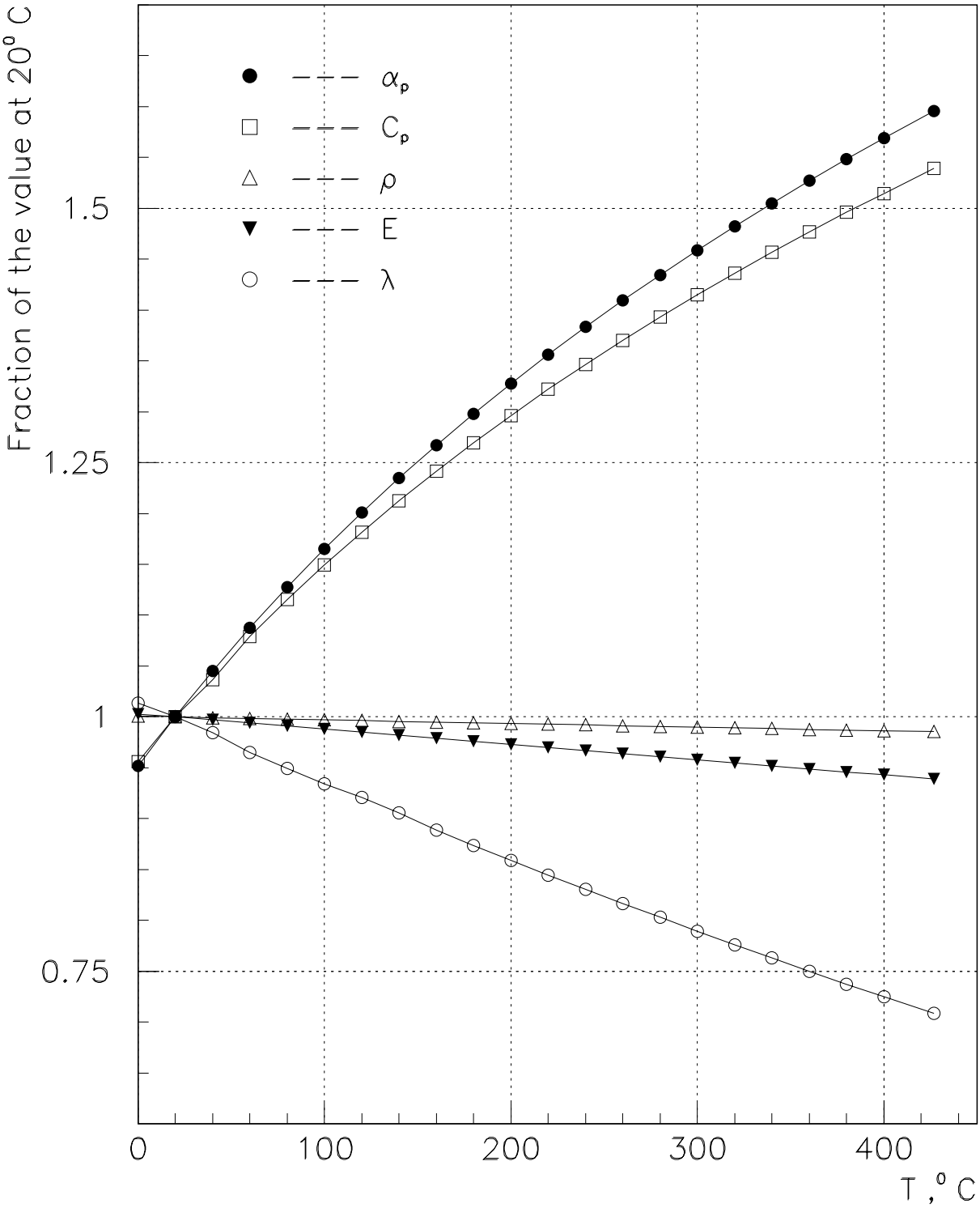

Figure 1.2: Temperature dependences of thermophysical and mechanical properties of beryllium.

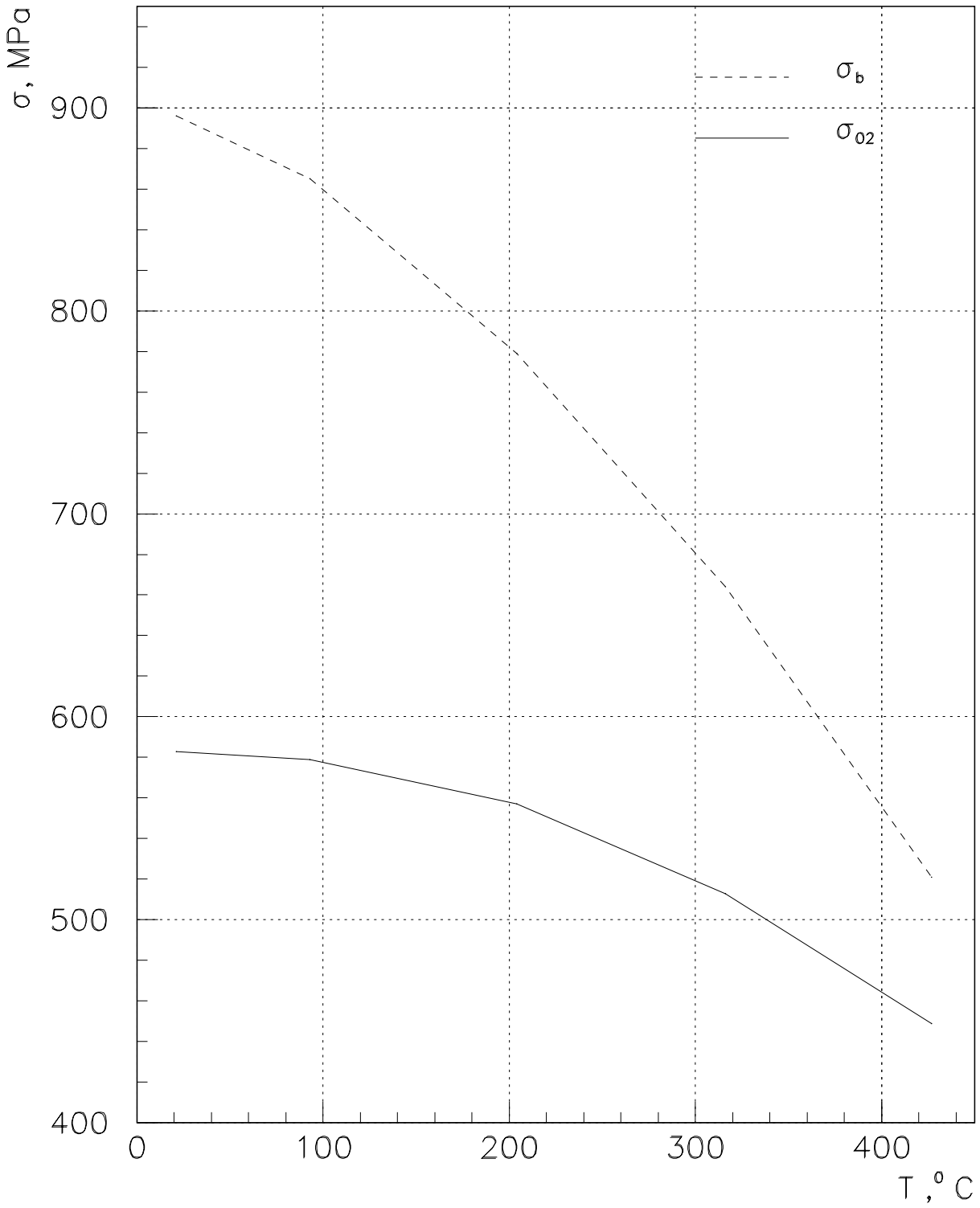

Figure 1.3: Tensile (- - -) and yield (—) strengths as functions of temperature for beryllium alloy I–400, modified and forged.

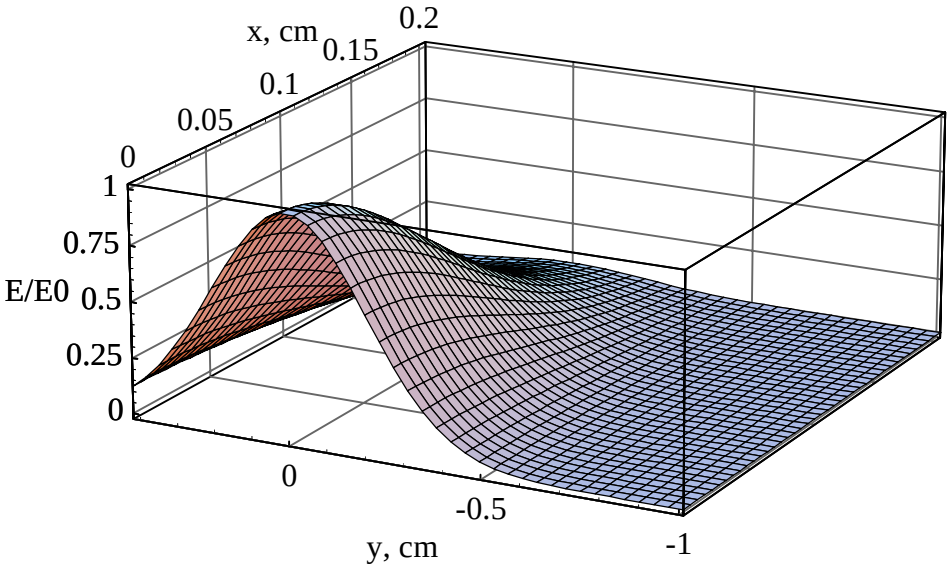

Figure 1.4: x, y–distribution of the energy deposition density in the beam region of the fin beryllium target (relative units).

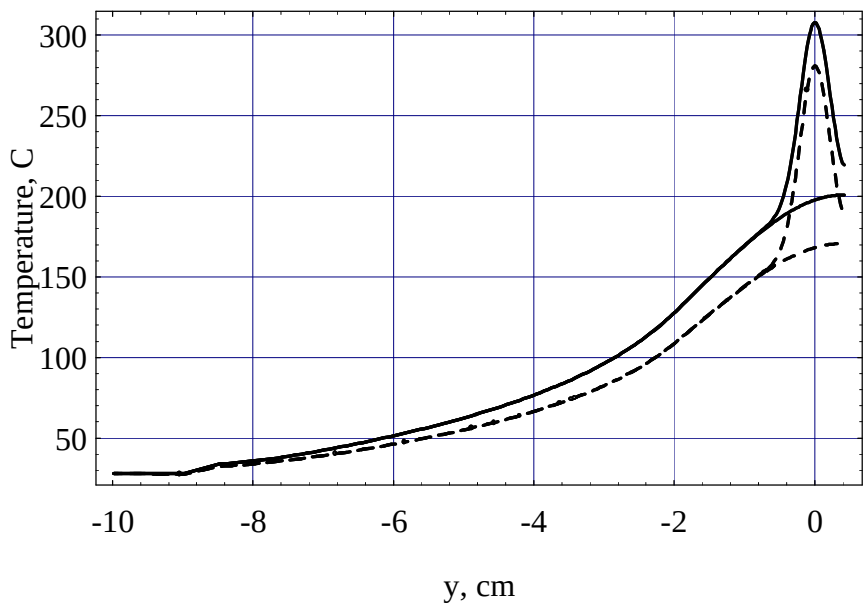

Figure 1.5: Temperature distributions in the target along y-axis ($x = 0$) just before and after the beam spill at a steady state. Solid lines correspond to the water cooling only; dashed lines correspond to the combined cooling: water, forced gas convection and radiation.

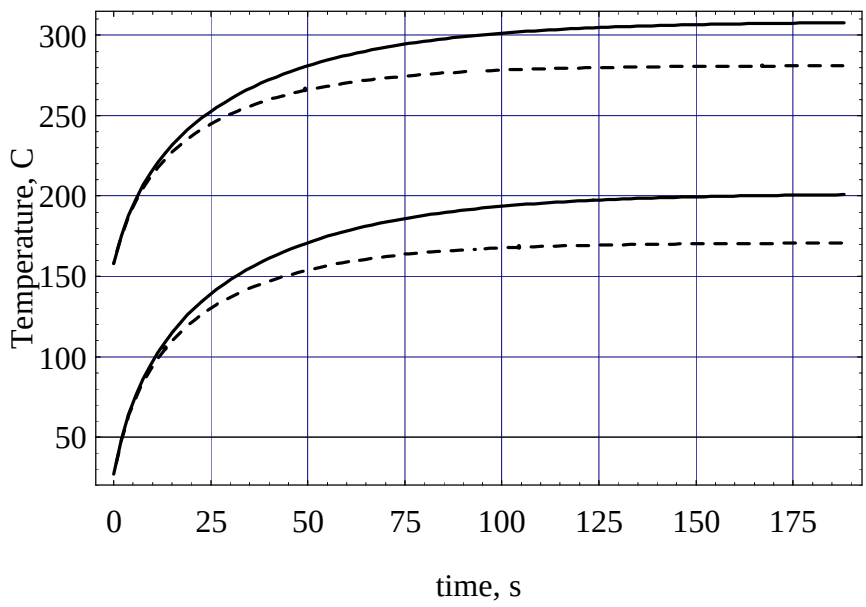

Figure 1.6: The evolution in time of the target temperatures for two methods of cooling (solid lines – water cooling only; dashed lines – combined cooling). The bottom and top curves correspond to the beginning and the end of the beam spill respectively.

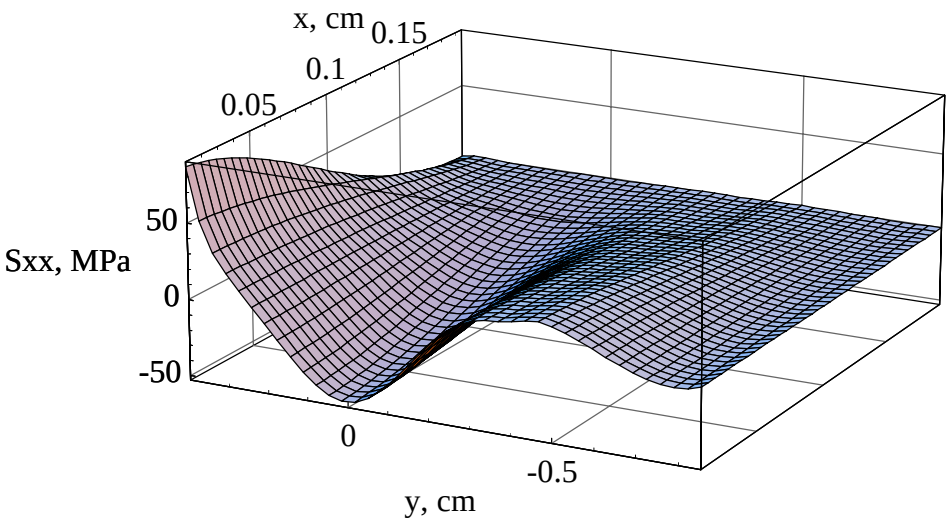

Figure 1.7: x, y–distribution of stress component σ_{xx} in the center of the beryllium fin target piece (L = 12 mm) just after the beam spill.

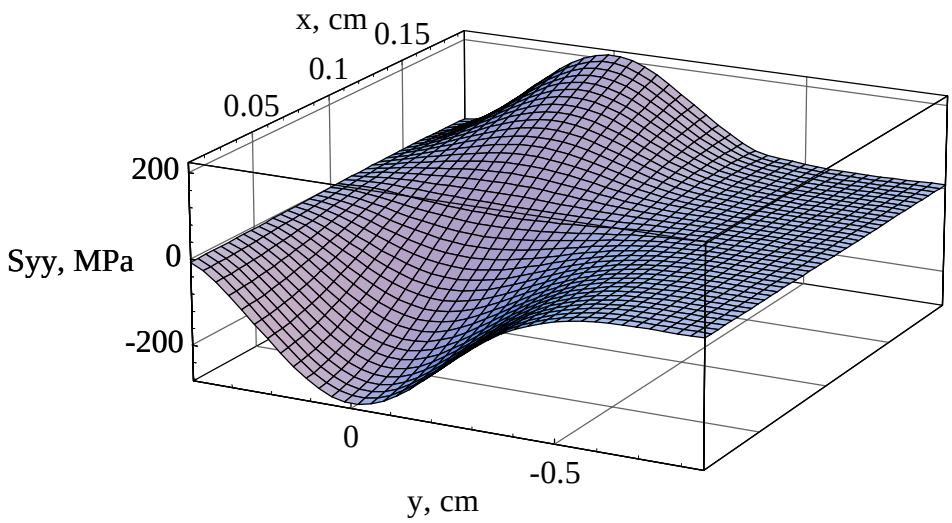

Figure 1.8: x, y–distribution of stress component σ_{yy} in the center of the beryllium fin target piece (L = 12 mm) just after the beam spill.

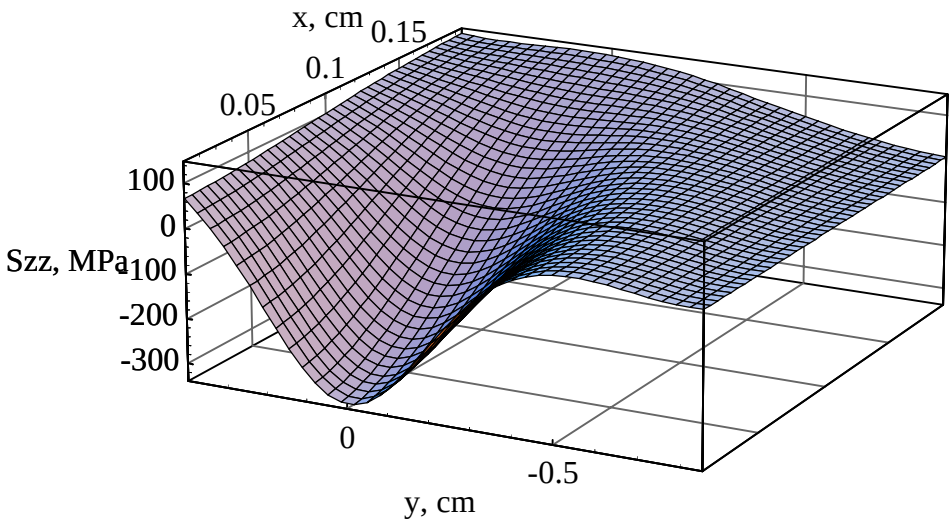

Figure 1.9: x, y–distribution of stress component σ_{zz} in the center of the beryllium fin target piece (L = 12 mm) just after the beam spill.

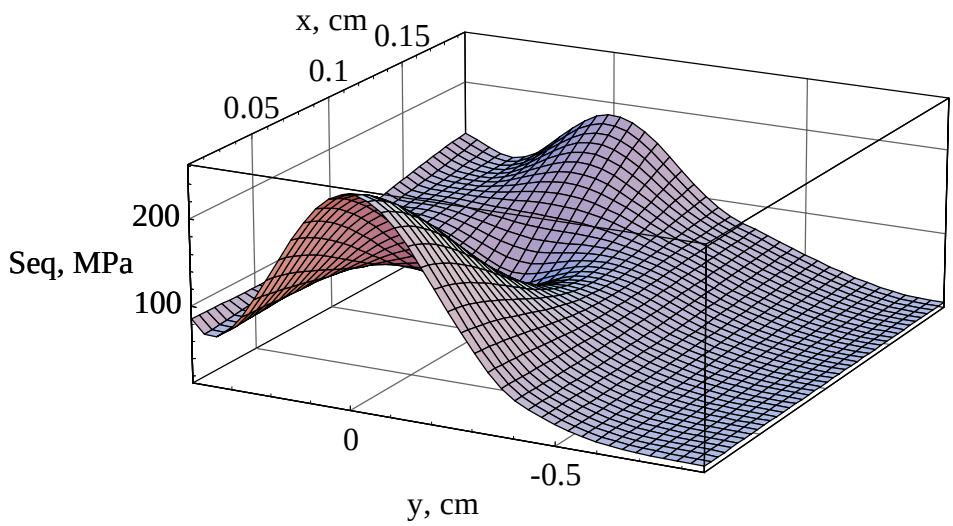

Figure 1.10: x, y–distribution of equivalent stress σ_{eq} in the center of the beryllium fin target piece (L = 12 mm) just after the beam spill.

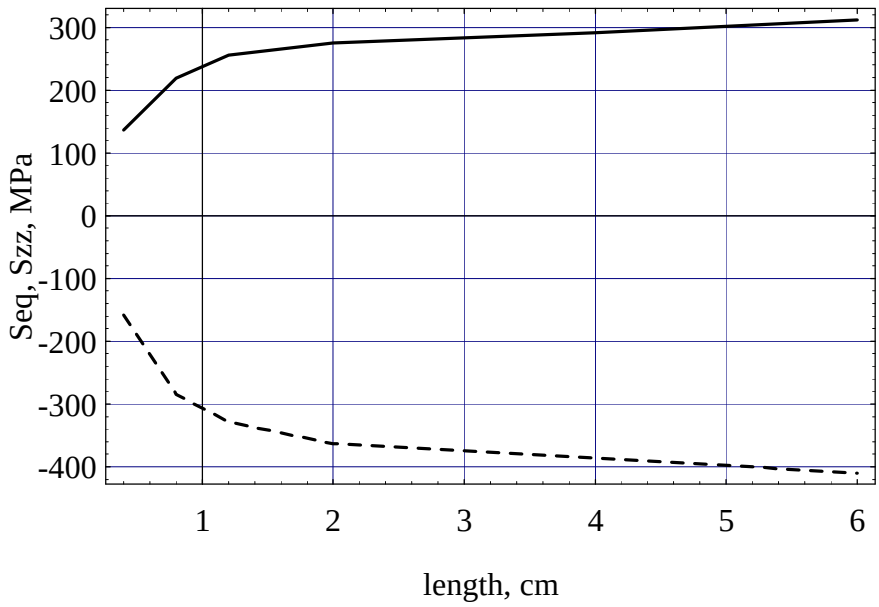

Figure 1.11: Equivalent stress σ_{eq} (solid line) and longitudinal stress component σ_{zz} (dashed line) at the point ($x = y = 0$, $z = \mathrm{L}/2$) just after the beam spill as functions of the target piece length.

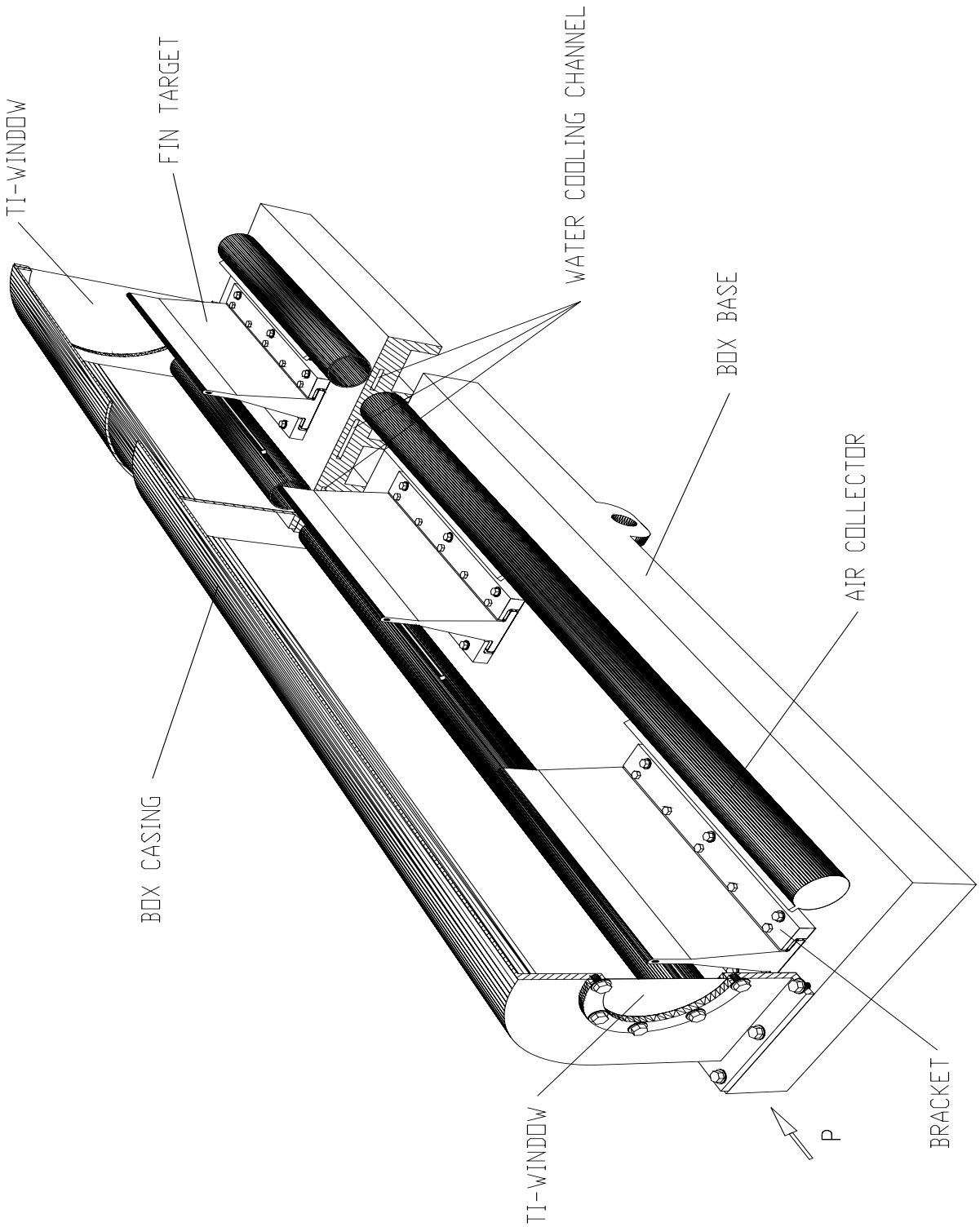

Figure 1.12: Perspective view of the target unit.

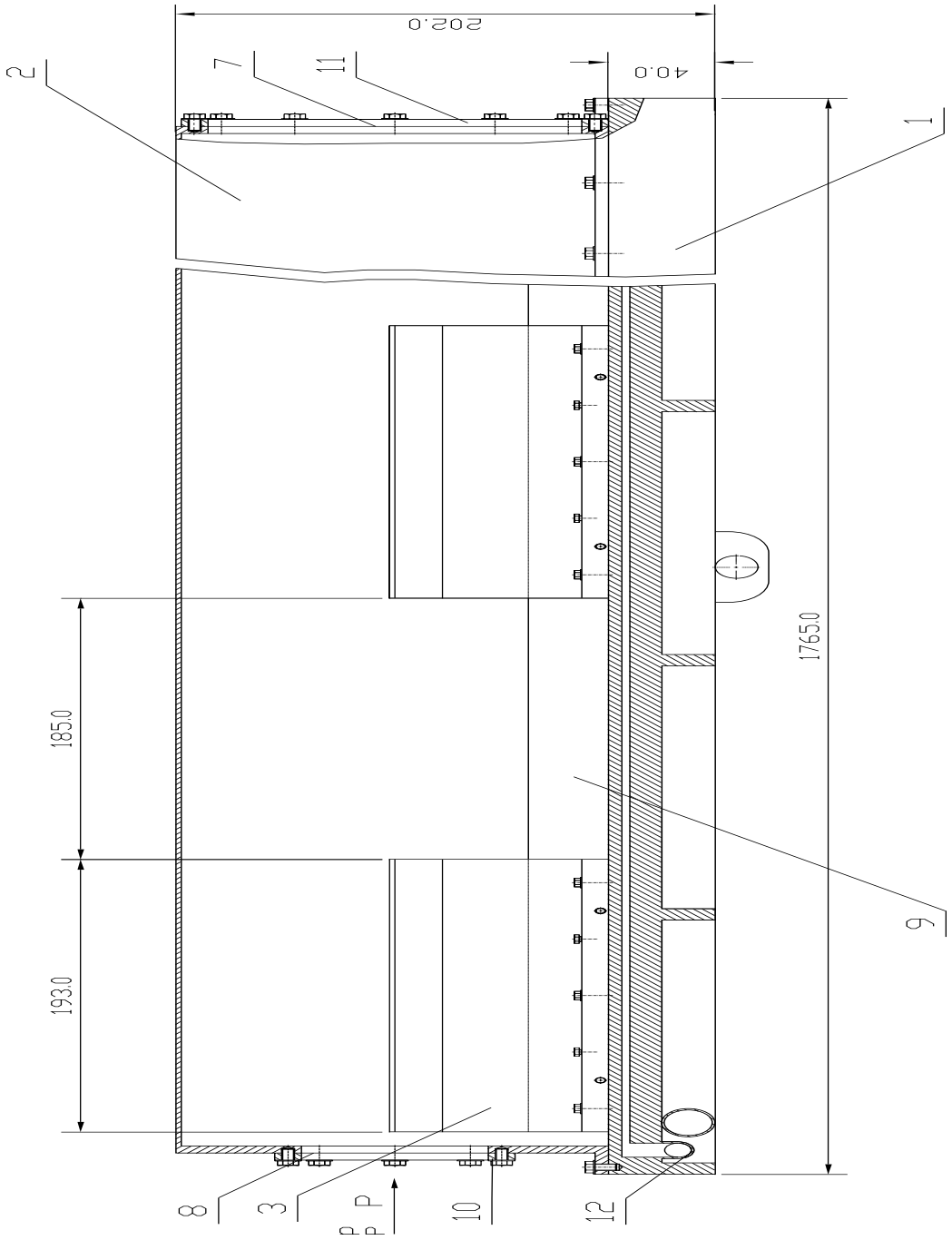

Figure 1.13: Side view of the target unit.

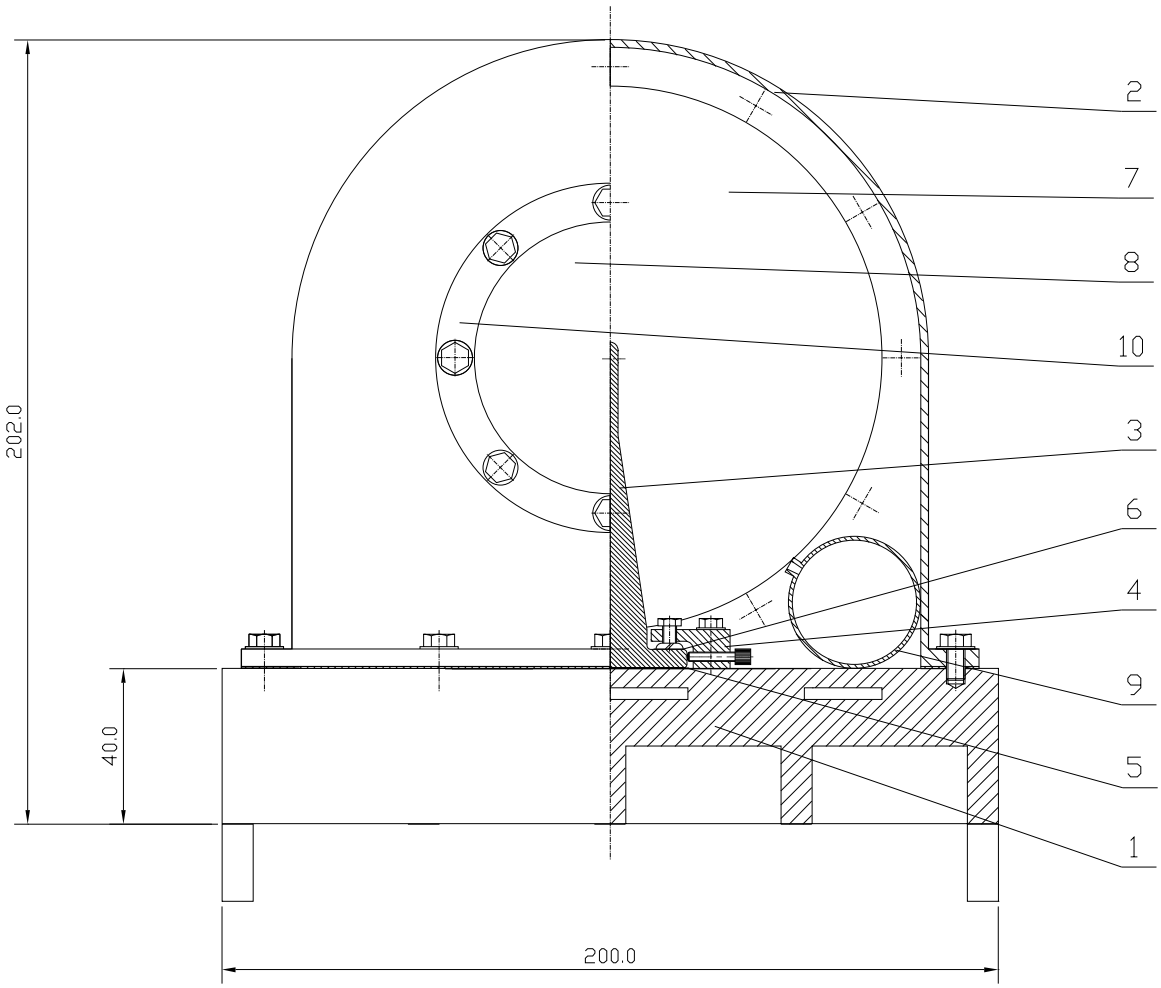

Figure 1.14: Front view of the target unit.

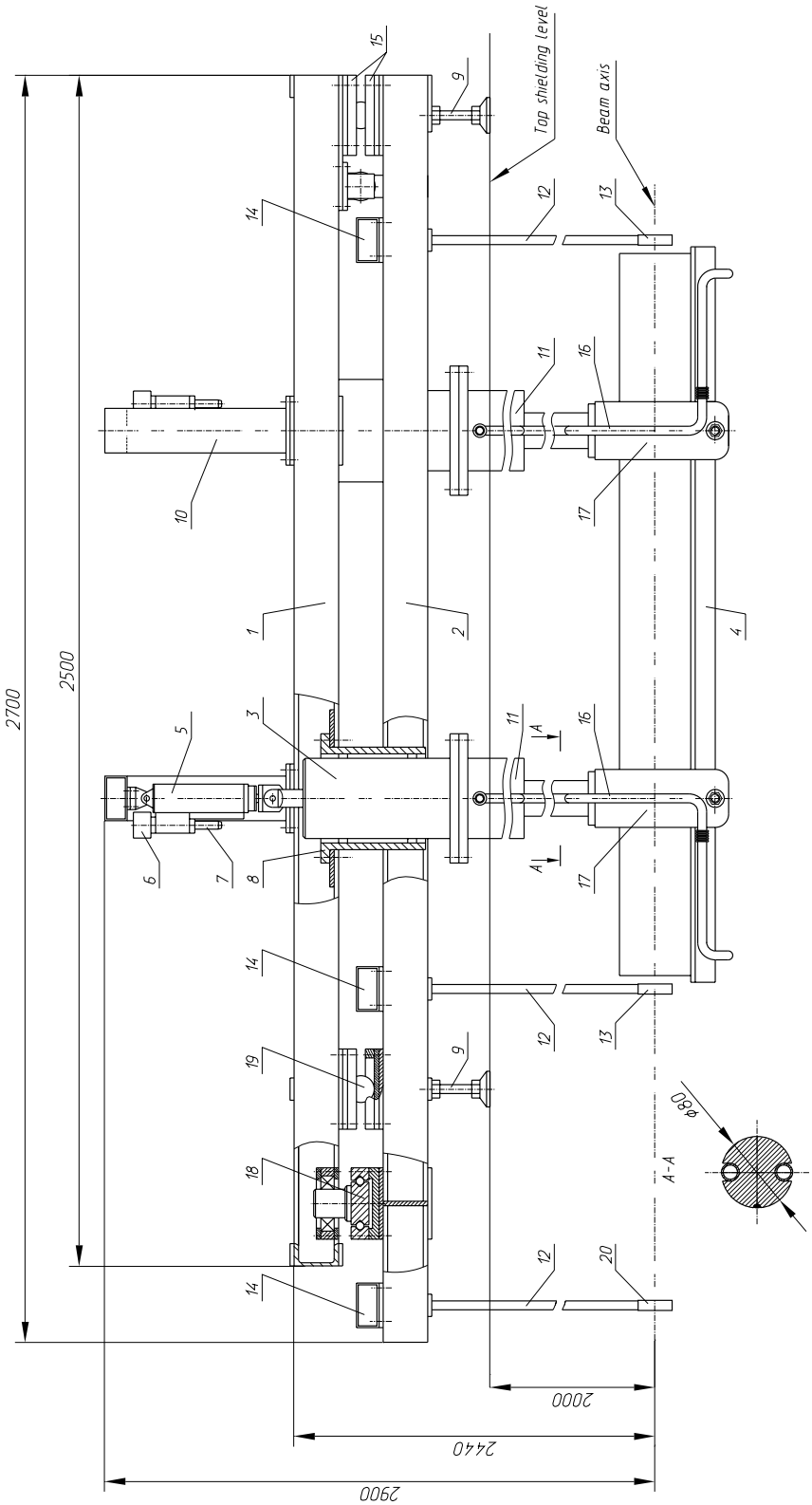

Figure 1.15: Side view of the alignment plant.

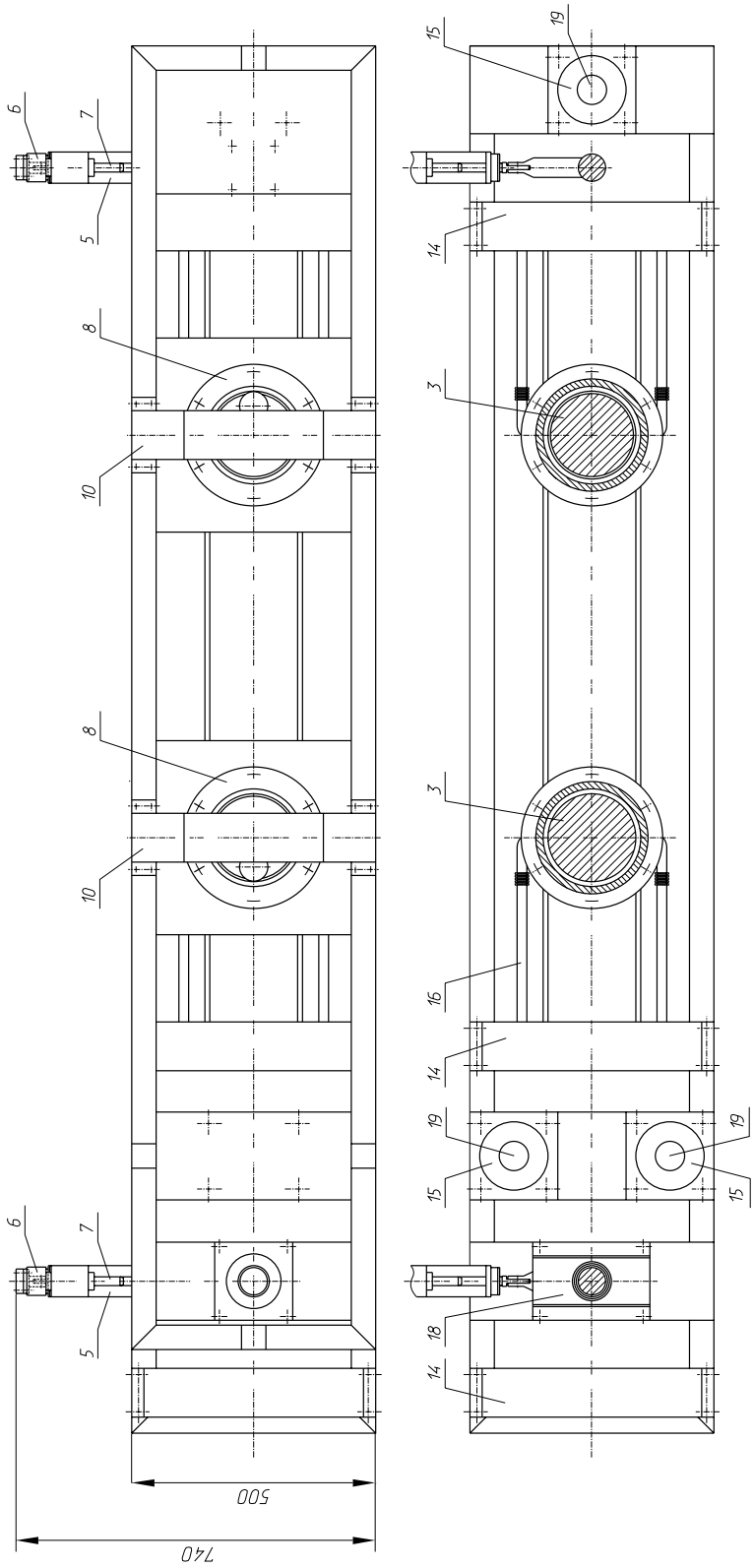

Figure 1.16: Top view of the alignment plant.

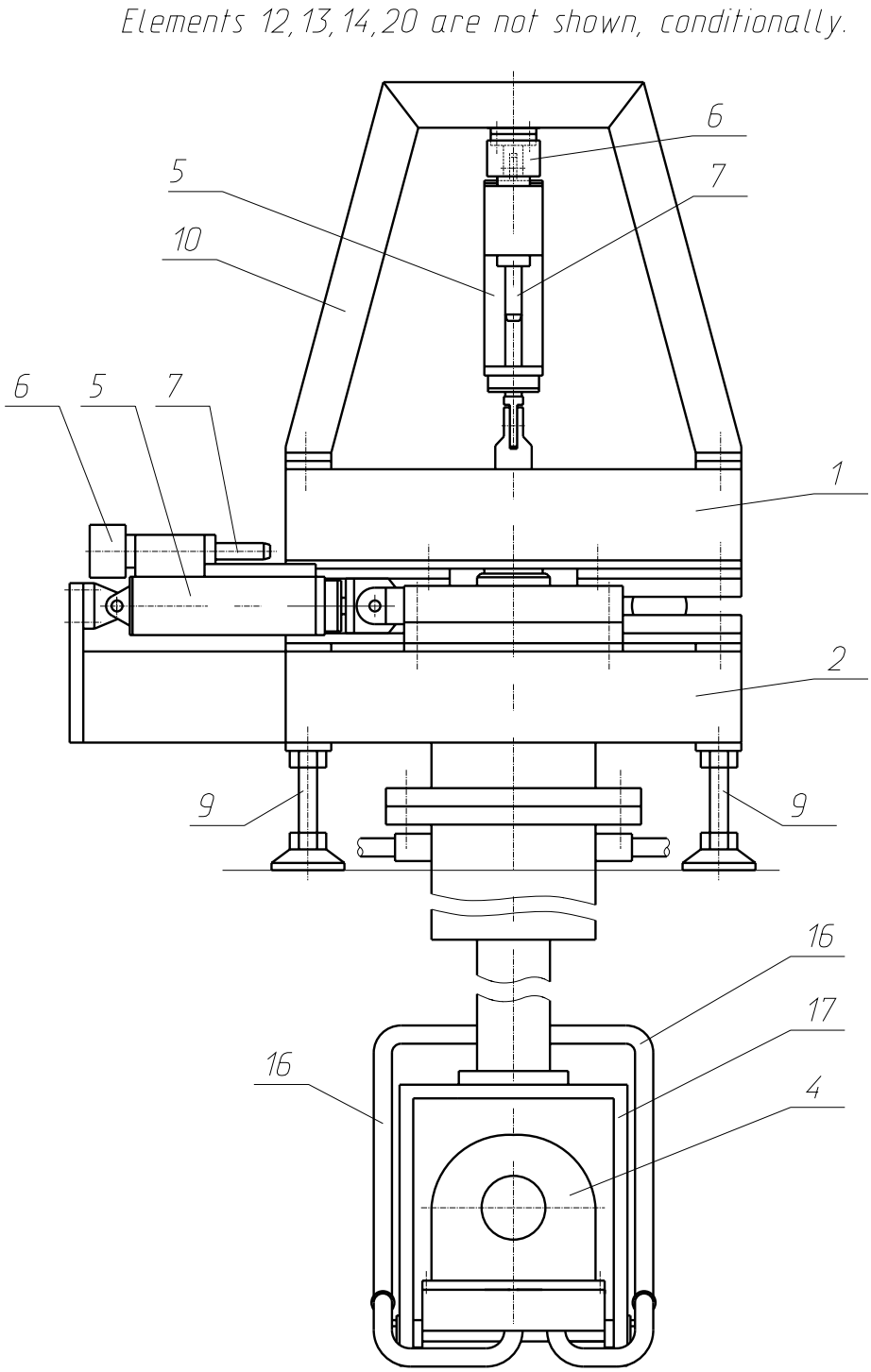

Figure 1.17: Front view of the alignment plant.

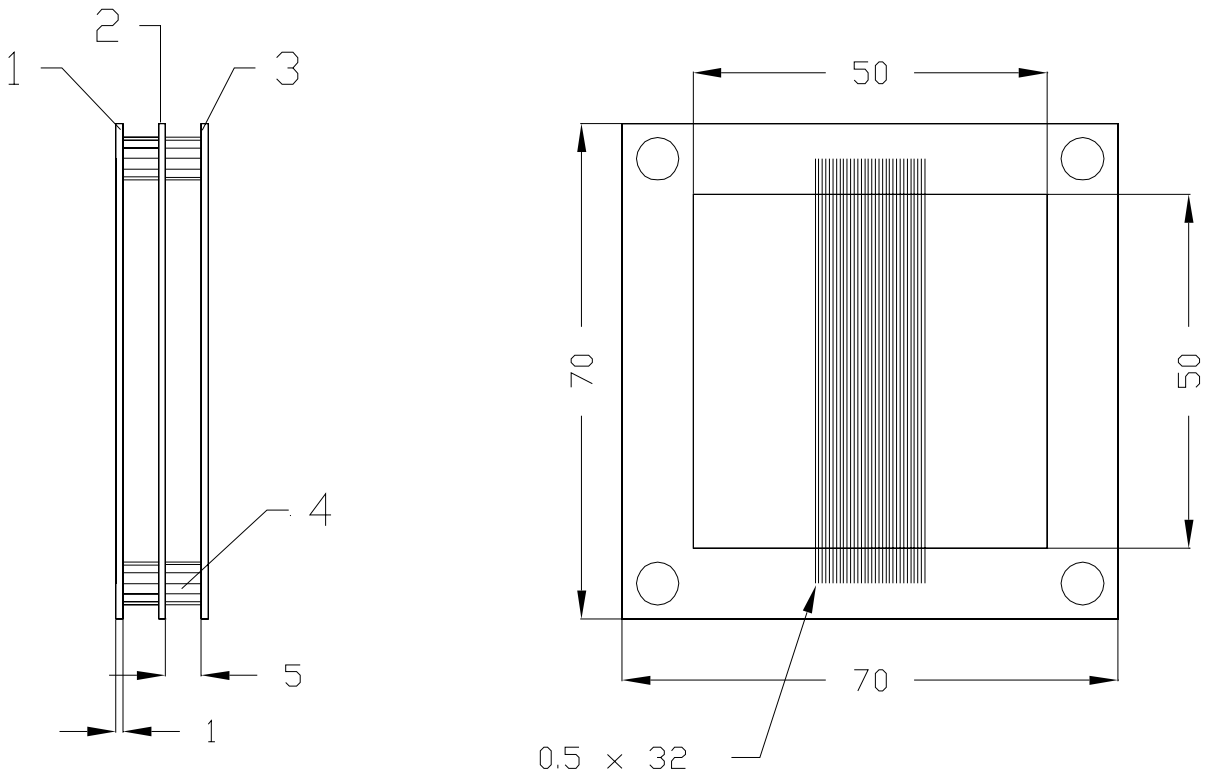

Figure 1.18: The secondary emission profilometer.

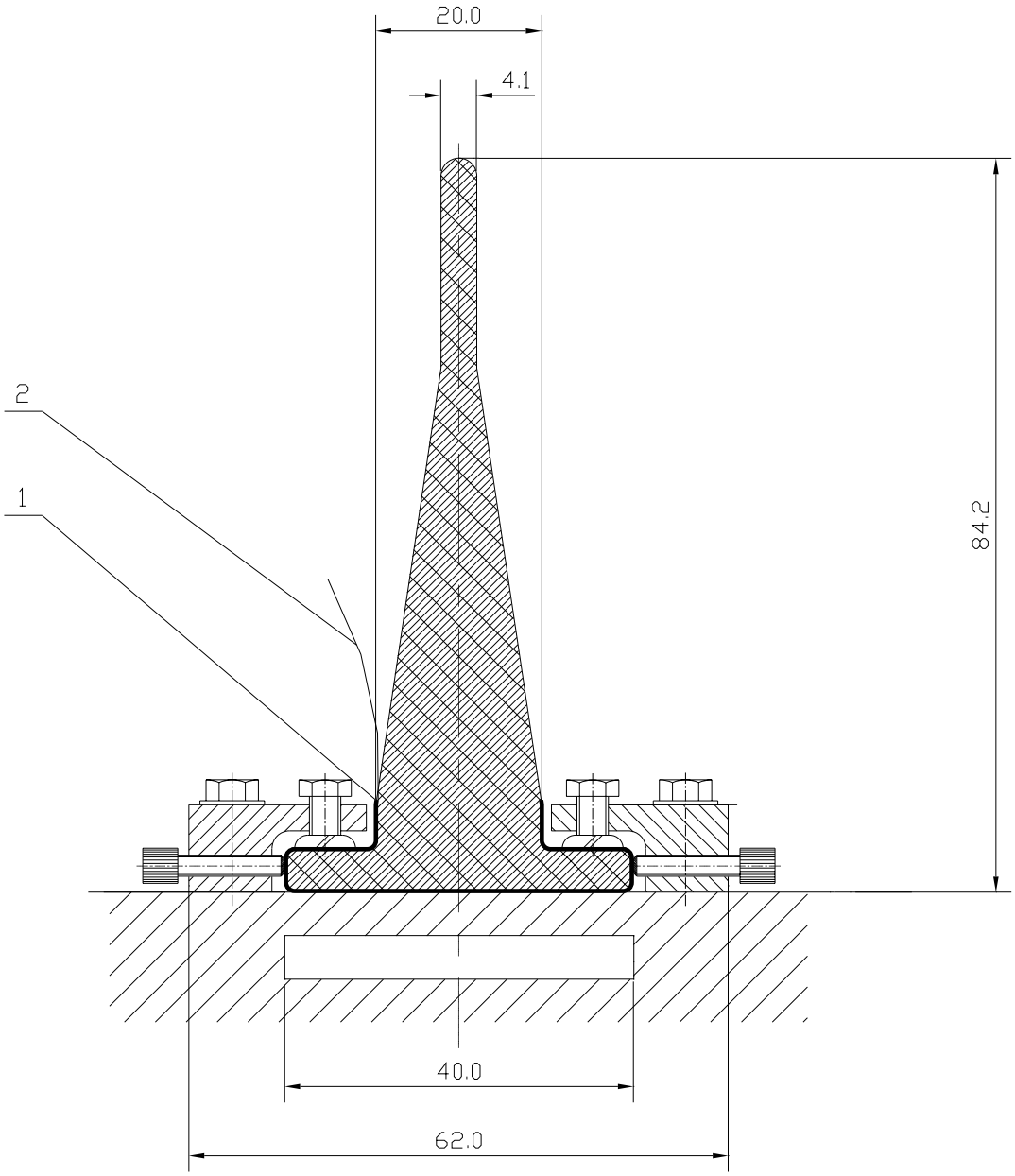

Figure 1.19: The insulated target.

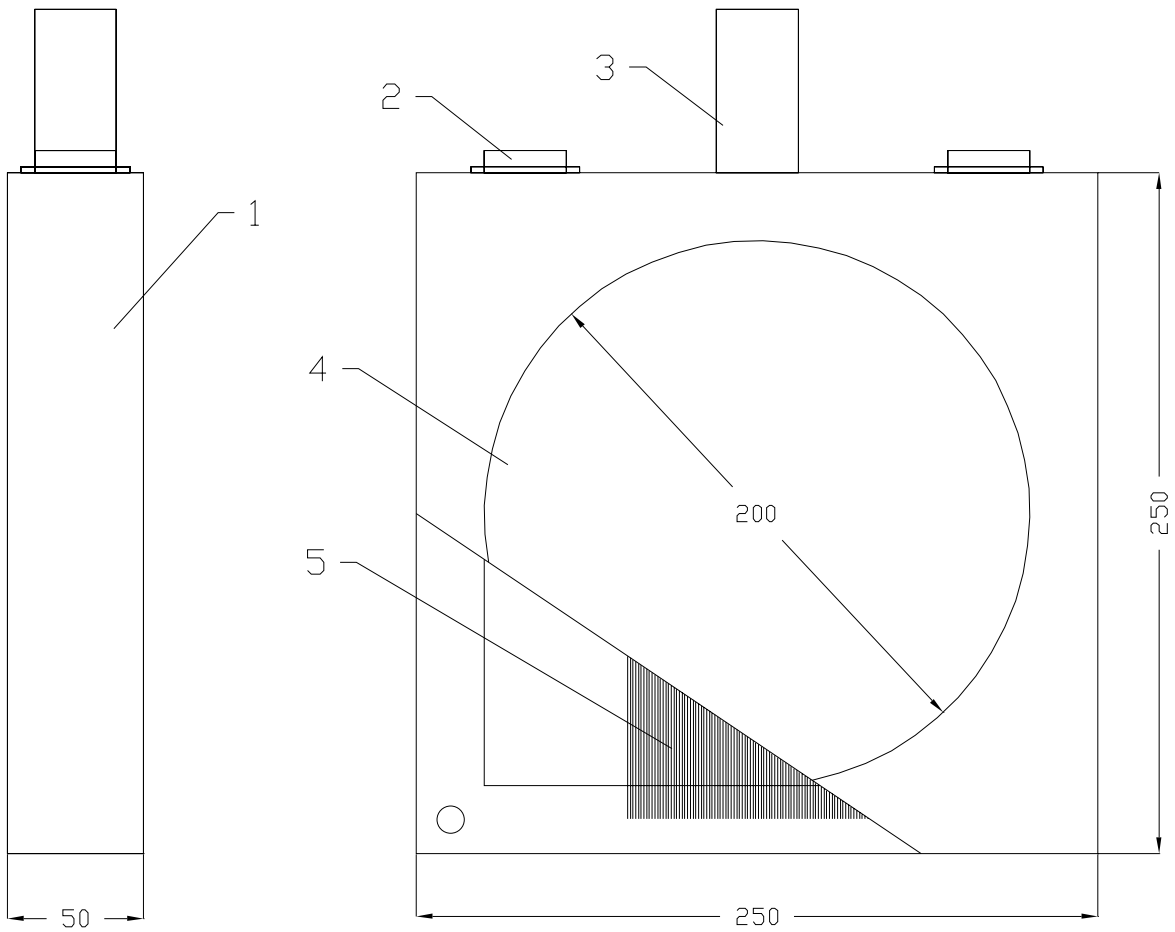

Figure 1.20: The large-aperture secondary emission profilometer.

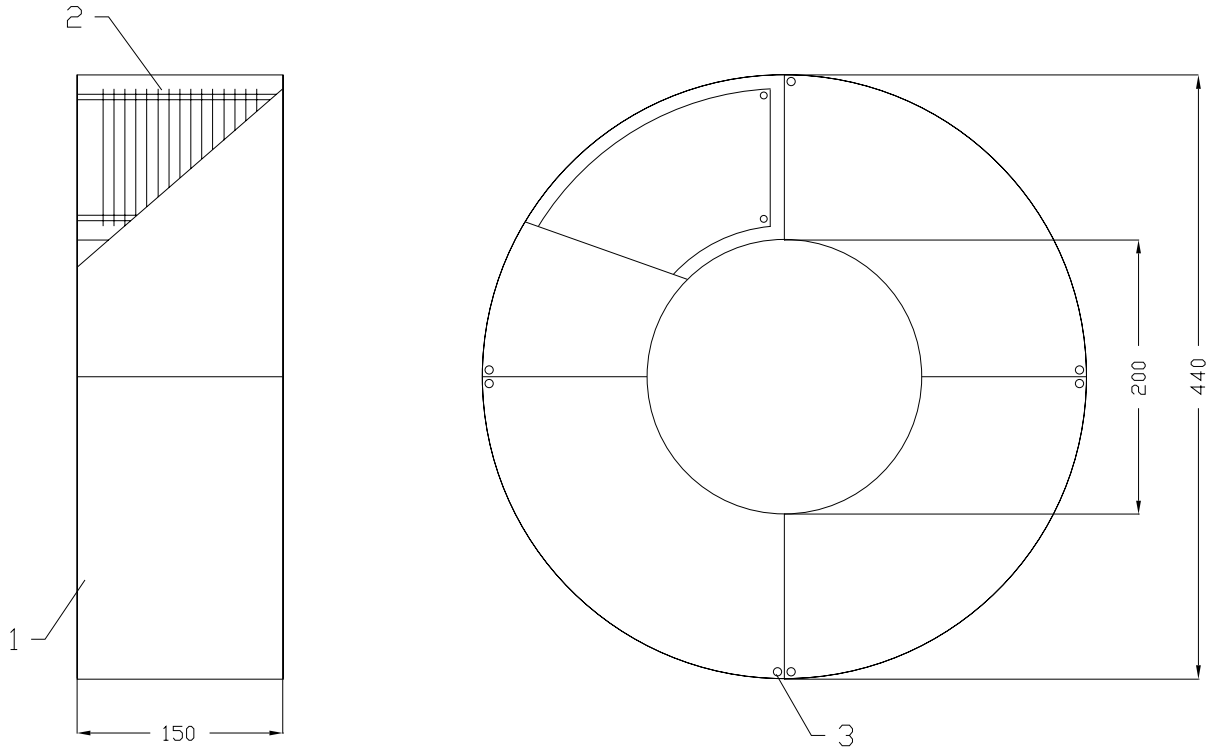

Figure 1.21: The split-plate ion chamber.

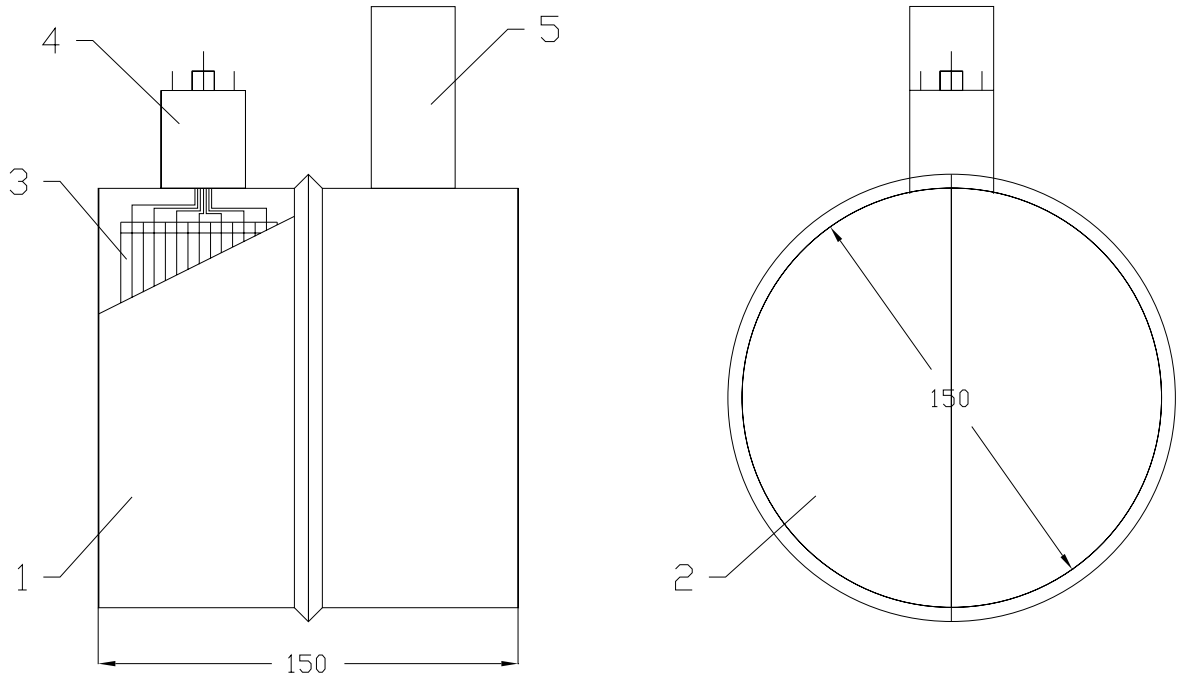

Figure 1.22: The secondary emission monitor.

2 NuMI Beam Focusing Systems with Conical and Parabolic Horns (preliminary results)

Focusing systems consisting of horns with parabolic shaped inner conductors (parabolic lenses) have been described in previous IHEP Reports [1] and [2] for the wide band and narrow band NuMI beams. The main advantages of a parabolic lens focusing systems compared with Fermilab baseline designs are the following:

- the usage of the same focusing devices (FD) and power supplies for both wide (WBB) and narrow (NBB) band neutrino beams;
- the inner conductors for parabolic lenses actually exist or they could be made using the existing process;
- the radiation shielding for the target station and focusing system, as well as the Target hall could be about 13 m shorter.

However, the neutrino energy WBB spectrum from the Fermilab H6.6 conical horns focusing system tends to be smoother than that from the parabolic lens, and be more suited for looking for oscillatory effects in the spectrum [6].

To obtain a more smoother shape of the WBB neutrino spectrum having all advantages of a parabolic lens focusing systems listed above, the beam optics with two conical V shaped inner conductors for the first FD and two parabolic shaped inner conductors L3 for the second FD has been preliminary studied. This new WBB focusing system labeled as 2LV/2L3 has the same z–locations for both FDs as the previous considered parabolic lens focusing systems. The currents in 2LV and 2L3 are equal to 260 and 320 kA respectively.

Each V shaped conical horn has the length of 1.28 m and the wall thickness increasing continuously from 2 mm near the flanges up to 6 mm in the neck region. The radius of the hole for passing of the proton beam is equal to 7 mm. Electrical parameters of 2LV focusing device are listed in Table 2.1. The main geometrical dimensions for the L3 lens and electrical parameters of 2L3 focusing device are given in previous IHEP Reports.

Inductance L, nH	450
Resistance R, μOhm	260
Peak current I, kA	260
Duty factor Q	780
Stored energy E, kJ	15.2
Average power P, kW	23
Power flux from the neck surface, W/cm^2	15.9
Neck temperature jump ΔT, °C	26

Table 2.1: Electrical parameters of the 2LV focusing device.

The neutrino energy spectrum and the total event rate at the far detector for the 2LV/2L3 focusing system compared with those for the H6.6 conical horns design calculated by Fermilab beam simulation package GNuMI are shown in Figure 2.1. The target for both WBB designs consists of eight 12.5 cm long graphite rods, each 2 mm in radius, separated by 8 cm long gaps. In this calculations the neck thickness for Horn 1 in H6.6 design was increased to 3 mm according to engineering study, as well as the magnetic field inside horn walls was taken into account.

The proposed focusing system with the addition of some dipoles and a proton beam dump can also be used to produce a narrow band beam. The neutrino energy spectrum and the total event rate at the far detector calculated by GNuMI for this system (labeled as 2LV/2B/2L3) in a case of 45 GeV/c tune are given in Figure 2.2. The 0.4 m long beryllium target with the radius of 2 mm was used for these beam simulations.

As follows from this Figure, there is no principal difference between the focusing properties of the 2LV/2B/2L3 system and 2LX/2B/2L3 system with parabolic shaped inner conductor for the FD1 described earlier. Besides, the ratio of the neutrino events with E <10 GeV (low energy tail) to the total number of neutrino events is equal to 0.36% for the 2LV/2B/2L3 focusing system with respect to 0.38% for the 2LX/2B/2L3 one.

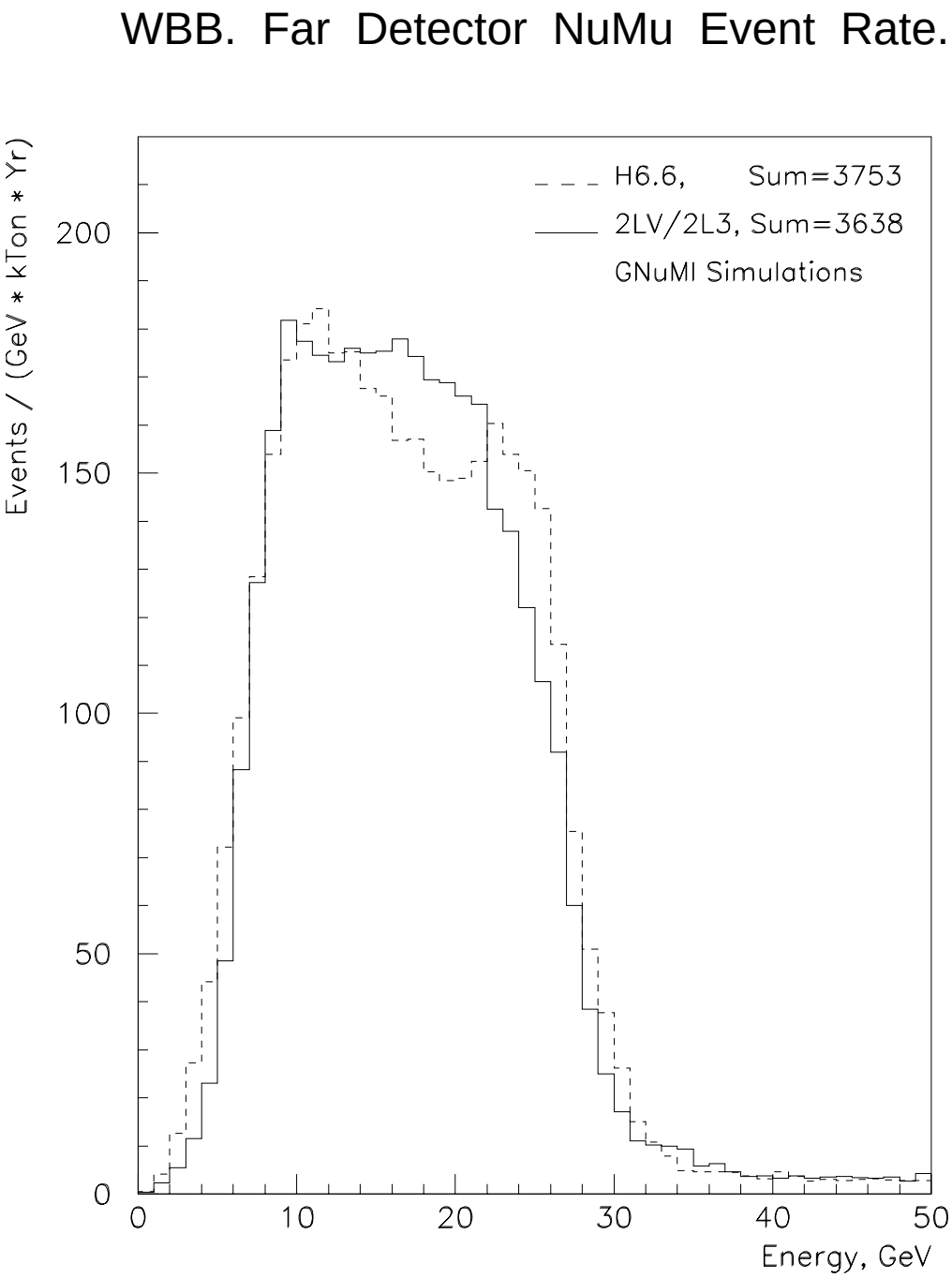

Figure 2.1: The ν_μ event rate for the 2LV/2L3 and H6.6 focusing systems.

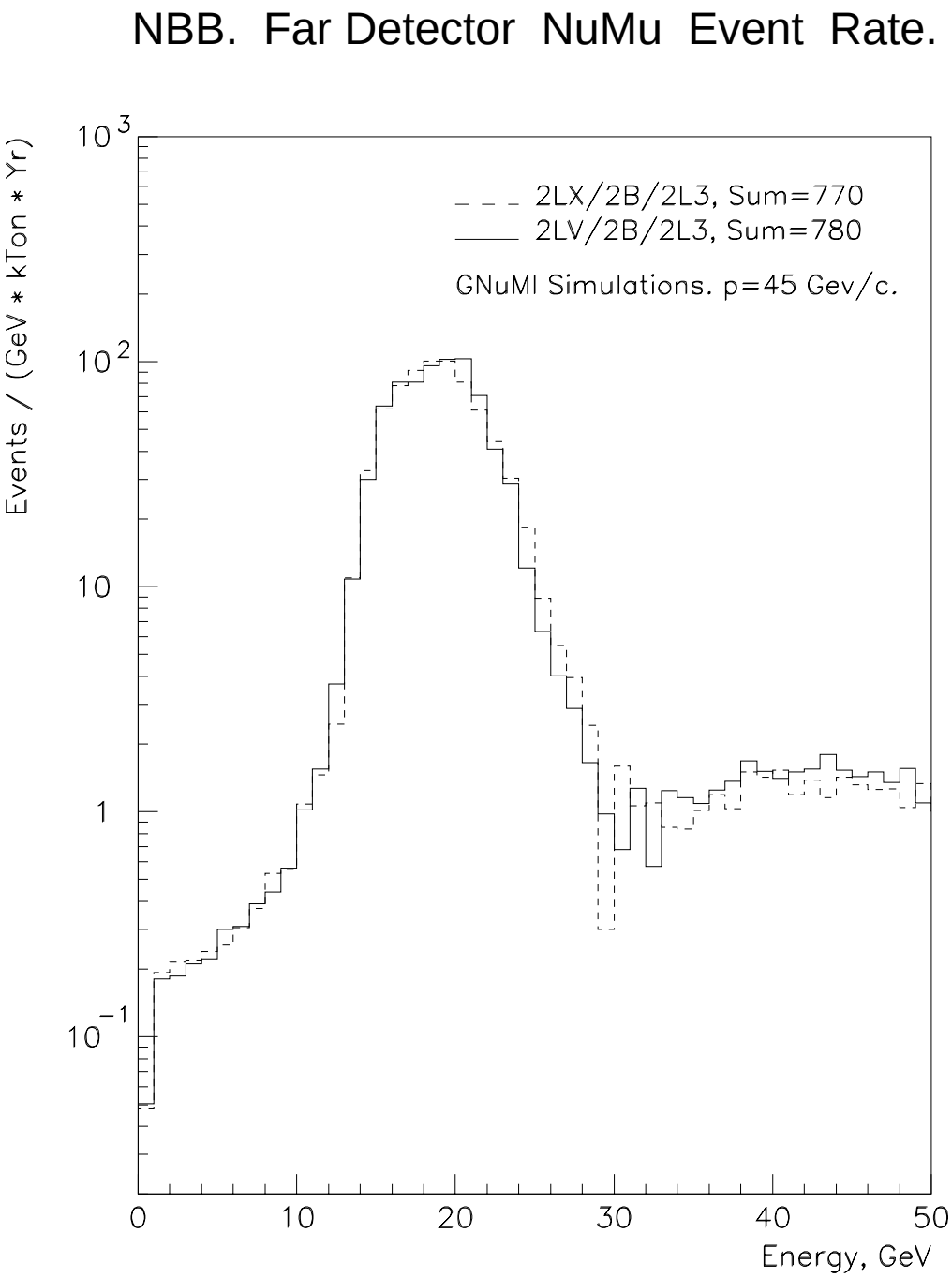

Figure 2.2: The ν_μ event rate for the 2LV/2B/2L3 and 2LX/2B/2L3 focusing systems.

3 Parabolic Lenses

In this Report the general layout of the WBB beam components in the case when power supply room has vertical disposition is described as well as one possible variant of the installation of FD on a beam line and replacement of failed FD without movable parts of a shielding are represented. Some details of FD assembly with its strip line, alignment system are given in 8 drawings being the first attempt to imagine how it looks.

3.1 General layout

Figure 3.1 is the general view of the Target Hall with the beam components for WBB and shielding in the case of the vertical disposition of the power supply room. The width of the Target Hall is equal to $\sim$ 6.6 m.

The transformers (each is 3.0 m height, 1.8 m length, 1.0 m width and 9700 kg weight) are placed in the Target Hall in order to minimize the strip line length. The position of the transformer feeding FD1 it seems to be unique providing easy installation and removal of FD1 and target. In this case the strip line lengths from the transformers to the focusing devices are equal to $\sim$ 6 m for FD1 and $\sim$ 5 m for FD2.

A discharge circuit is distributed over four cabinets, placed in a power supply room. Each cabinet contains 25 capacitor banks, thyristor switch and 7–th harmonic correction circuit. The sizes of cabinets are: length — 1.9 m , width — 1.0 m, height — 1.7 m. and weight — 1800 kg. The primary side of the transformer is connected to the discharge circuit via several parallel cables. The type and quantity of a cable will be defined during the design study of a power supply.

The configuration of the Target Hall with FD is shown in Figure 3.2 and the cross–section along the beam line in Figure 3.3. The focusing device with its strip line and water cooling pipes is fastened to the mounting table, the desk of this table as well as the vertical rods being the parts of a shielding. The vertical rods are fastened to the horizontal alignment frame; the connection between vertical rods and FD mounting table is provided with long vertical screws passing inside the rods. The strip line passes through the shielding via special labyrinth in order to prevent the radiation exposure of the equipment placed at the top of the shielding.

Such configuration is chosen in order to refuse of the movable parts of the

shielding (see [2]). In this case the initial installation of FD and removal of the failed components are rather different from that described in a previous Report [2]. Some details of the FD assemblies with an alignment table are shown in the drawing Y7150-00-00-00 (2 sheets) and Y7151-00-00-00 (see Attachment).

3.2 Initial Installation of FD and Replacement of failed FD assembly

The initial installation of focusing device to the beam line may be done with the following procedure:

- The vertical alignment frame is installed to the proper location and aligned in a horizontal plane; two vertical guideway rods are fastened on a frame.
- The assembly of mounting table with FD, vertical supporting rods, horizontal alignment frame and strip line should be carefully balanced in all directions by means of the counterweight placed at a lower part of a table desk to relieve the mounting and replacement of FD. This assembly is placed on the vertical alignment frame by overhead crane; two holes in a horizontal alignment frame together with two vertical guideway rods mentioned above will prevent the rotation of the assembly during lowering (lifting).
- The FD is aligned to the beam axis. The information about the position sensors state is put into a memory. The power, water and instrumentation are connected and tested.
- The whole assembly is lowered by means of vertical alignment system until the table legs touch of the Target Hall floor. The special system to detect if the legs touch of the Target Hall floor should be designed.
- The horizontal alignment frame with vertical supporting rods is disconnected from the mounting table with long vertical screws. The vertical screws are taken out.
- The horizontal alignment frame with vertical rods is lifted.
- The shielding blocks with proper holes are placed to their positions.

- The horizontal alignment frame with vertical supporting rods is placed to the vertical alignment frame, clamped with long screws mentioned above to the mounting table. The FD is aligned to the previous position by the vertical alignment system.

The replacement of failed FD assembly is nearly opposite to the installation:

- The location of all connections at the top of the shielding means, that for well designed shielding, there is personal access to the connections. Upon entering the hall (in a few days after beam off) all of the connections of power, water and instrumentation will be disconnected at the top of the shielding.
- The whole assembly is lowered by means of vertical alignment system until the table legs touch the Target Hall floor.
- The horizontal alignment frame with vertical supporting rods is disconnected from the mounting table with long vertical screws. The vertical screws are taken out.
- The horizontal alignment frame with vertical rods and shielding blocks are lifted and put in a place far enough from the personnel to provide minimal exposure.
- Special lifting fixture is attached to the FD mounting table, and the whole assembly is lifted and placed to a coffin.
- Following procedure of the installation of spare unit is practically similar to initial one, but may be slightly different because of residual activity of the shielding walls when the shielding blocks above the FD are removed. The special tools should be designed to clamp the vertical screws for connection (disconnection) of vertical supporting rods to the mounting table in order to prevent the exposure of personal.

3.3 FD assembly

The assembly of the first focusing device (2LX) with its strip line and flexible connection is shown at drawings Y7150-01-00-00 (4 sheets) and of the FD2 (2L3) assembly at drawing Y7151-01-00-00 (see Attachment to this Report). This is the first attempt to imagine how it looks. Both assemblies

take into account the IHEP neutrino beam facility experience except of flexible connection and water cooling system.

3.3.1 Inner conductor

Inner conductor for both focusing devices consists of two parabolic lenses, bolted together with help of several screws as it is shown in Y7150-01-00-00. The parabolic lens is machined out from the casting of aluminum alloy B2243–8, produced by "MOLNIYA", Moscow. The properties of this alloy are given in IHEP Report [1]. Each casting consist of 3 parts (two identical lateral and one symmetrical central parts) welded together in the atmosphere of neutral gas. The quality of each part of a casting as well as the welding joints are carefully checked by X–ray detection. The machining is produced by NC turning with a radial accuracy better than 0.1 mm and a maximum ovality default of 0.05 mm. The thickness of connecting flanges is equal to 15 mm.

3.3.2 Outer conductor

Outer cylindrical conductor with a wall thickness of 10 mm is an assembly of 3 parts screwed together. Each part is made out of metal sheet rolled and welded. The inner diameter of the outer conductor is 200 mm for FD1 and 520 mm for FD2 and is machined with a maximum ovality default of 0.2 mm. There are no special requirements to the outer conductor material. It may be made of high conductivity aluminum, well welded.

The junction of inner and outer conductors from the short circuit side is provided via two half rings and collet sleeve in order to prevent any prestress (stretched or compressed) of the shell of inner conductor during the assembly of FD and in the same time to provide the rigid joint (see drawing Y7150-01-00-00). The similar junction but without a collet sleeve is used from the current input side. Centering of the inner conductor with respect to the outer conductor is provided with three screws as it is shown in drawing Y7150-01-00-00. The insulation between the screws and inner conductor may be achieved, for example, with help of thin alumina sheet between the screw and the flange, or the layer of plasma sprayed alumina at the end of the screws.

The current feeding of FD1 is produced from two symmetrical sides via wide flange. The ANSYS analysis shows that if the diameter of this flange

is rather large with respect to the diameter of inner conductor (2 times in our case) the axial nonuniformity of current density near the flange does not exceed 1%. In the case of FD2 the axial uniformity of current density is achieved by the feeding of the inner conductor via part of the outer conductor which thickness is greater then two skindepths (in our case 24 mm, skindepth for aluminum is equal to 8 mm), as it is shown in the drawing Y7151-01-00-00. The length of the outer conductor with increased thickness should be equal at least to the input diameter of the inner conductor. The insulation of current input as well as the strip line part closed to the FD should be radiation resistant. The most suitable is alumina. IHEP has a good experience with the plasma sprayed alumina.

The flexible connection is made of aluminum grid as it is shown in drawing Y7150-01-00-00 (sheet 4). Each strip of the feeder is terminated by 45 aluminum wires, 5 mm in diameter. Each wire is welded to the aluminum piece, bolted to the strip. Only one flexible connection is planned to be used between the transformer and FD as the total length of the strip line is not very large (5–6 m).

3.3.3 Water cooling

The inner conductor is water cooled by spraying continuously of low conductivity water through the holes in the outer conductor from the three pipes (see drawing Y7150-01-00-00, sheet 3). The water cooling system should provide the heat transfer coefficient from the inner conductor surface of 6000 for FD1 and 2000 $W/m^2/°C$ for FD2. Preliminary analysis of a jet cooling [7] gives the values of the water drops density of 1.5 for FD1 and 0.5 $kg/m^2/s$ for FD2, and the velocity of water drops should be at least 10 m/s. Taking into account the values of surfaces of the inner conductors it corresponds to the total amount of cooling water of 80 for FD1 and 90 l/min for FD2. As for the jet cooling of a "cold wall" its estimation isn't very accurate yet, so the special measuring at the model has to be carried out.

The water is collected by gravity into a tank located below FD on the beam line. As the water jet is broken it is very difficult to have closed water cooling circuit. On this reason the water circuit is an open circuit where the pump sucks the water from the recuperation tank and spray it on the inner conductor. The pump pressure as well as the type and distribution of the nozzles will be defined after measuring at the model.

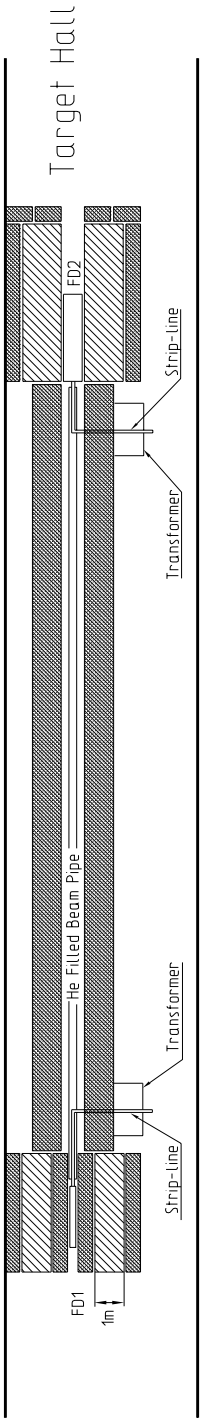

Figure 3.1: General view of the Target Hall.

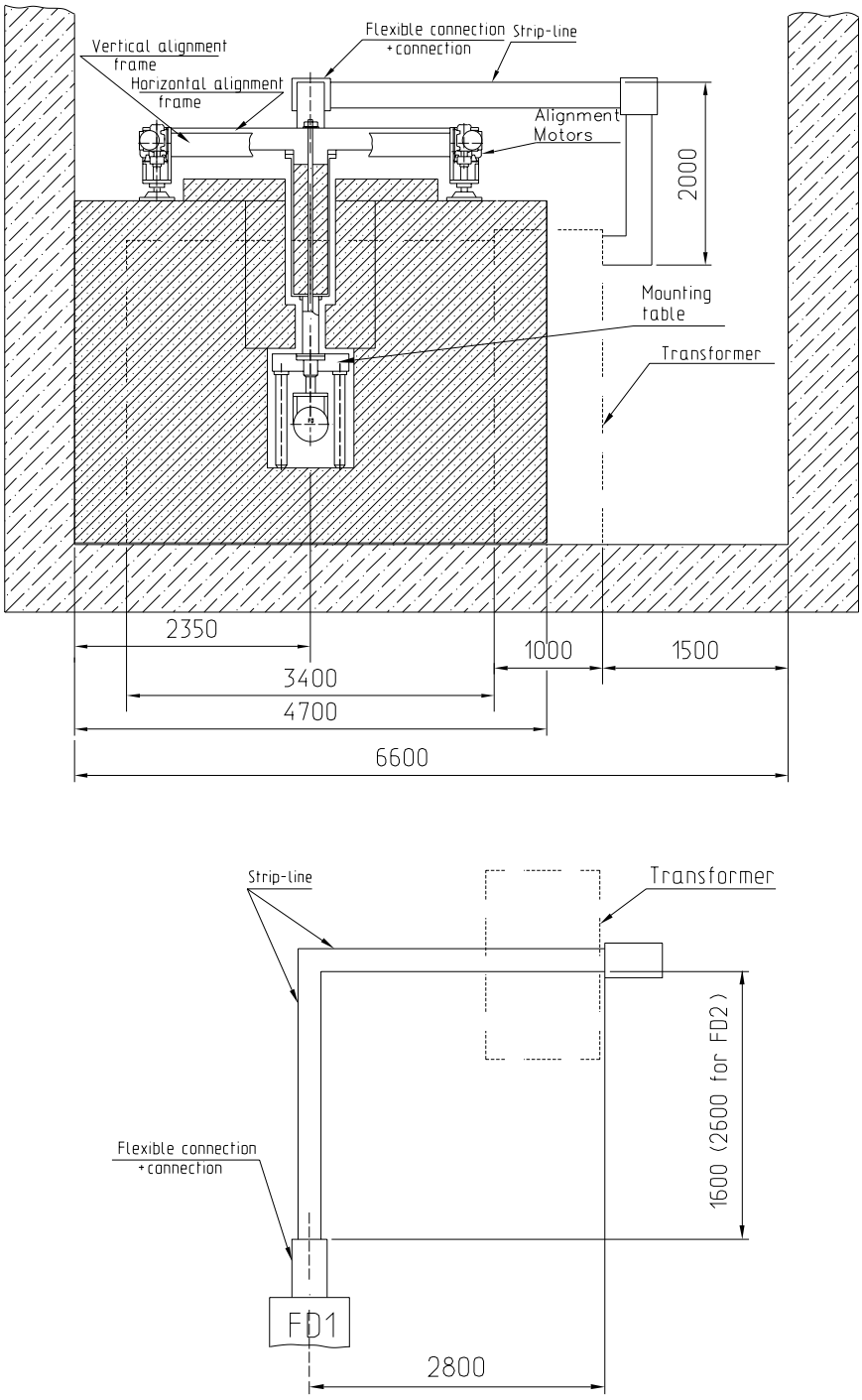

Figure 3.2: The configuration of the Target Hall with FD.

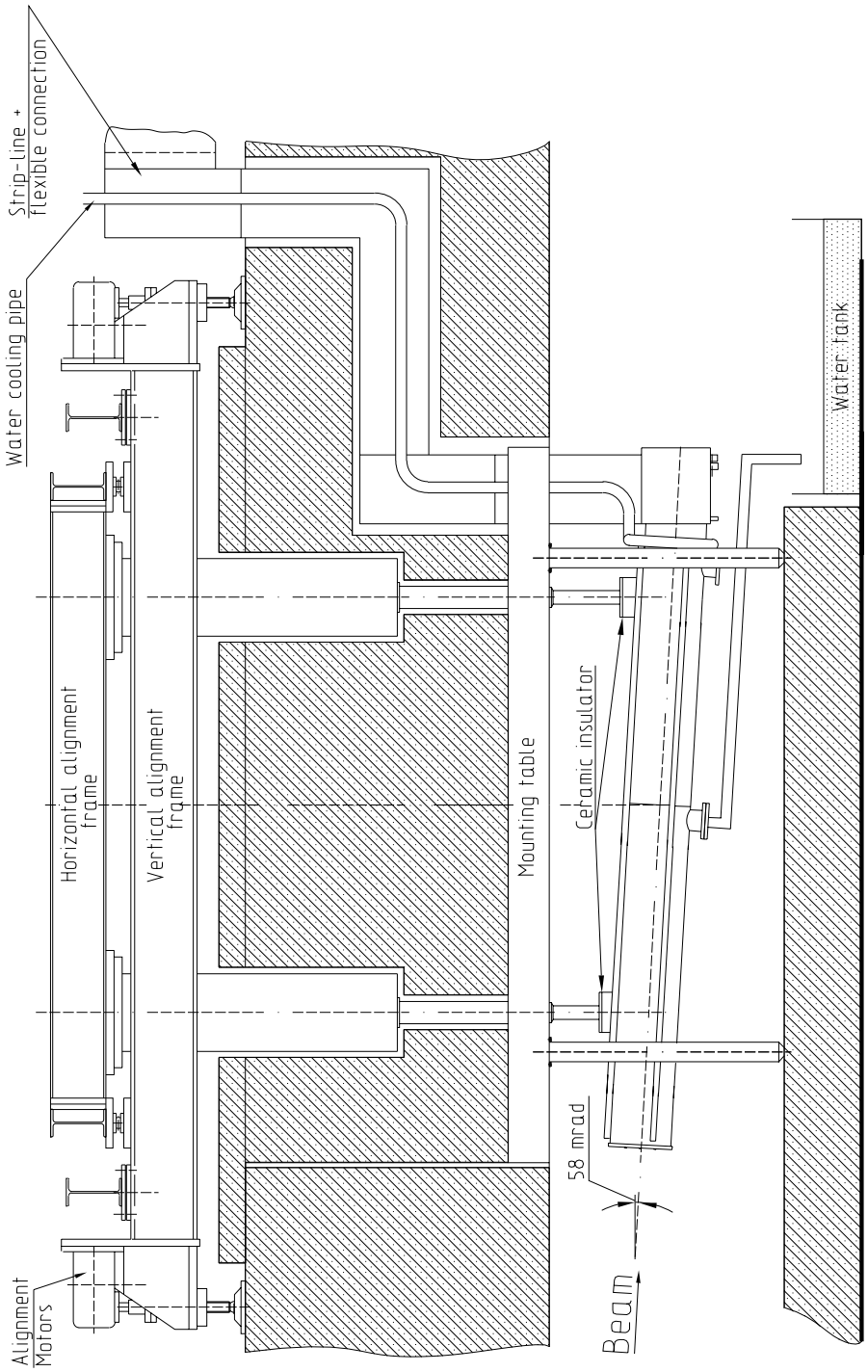

Figure 3.3: Cross-section of the FD assembly along the beam line.

References

[1] Preliminary Design Work and Neutrino Beam Calculations for the NuMI Project, IHEP, Protvino, 1997.

[2] Conceptual Design Work and Neutrino Beam Calculations for the NuMI Project, IHEP, Protvino, 1997.

[3] N.Mokhov, FERMILAB-TM-628, Batavia, 1995.

[4] A.Abramov et al, IHEP Preprint 84-64, Serpukhov, 1984.

[5] Status Report: Technical Design of Neutrino Beams for the Main Injector (NuMI), NuMI-B-92, (TM-1946), Batavia, 1995.

[6] Conceptual Design for the Technical Components of the Neutrino Beam for the Main Injector (NuMI), NuMI-B-285, Batavia, 1997.

[7] V.P.Isachenko, V.I.Kushnirev "Jet cooling", Energoatomizdat, Moscow, 1984 (in Russian).